

Kent Academic Repository

Full text document (pdf)

Citation for published version

Froebrich, Dirk (2017) New Compact Star Cluster Candidates in the Galactic Plane. Monthly Notices of the Royal Astronomical Society, 469 (2). pp. 1545-1552. ISSN 0035-8711.

DOI

<https://doi.org/10.1093/mnras/stx938>

Link to record in KAR

<http://kar.kent.ac.uk/61356/>

Document Version

Author's Accepted Manuscript

Copyright & reuse

Content in the Kent Academic Repository is made available for research purposes. Unless otherwise stated all content is protected by copyright and in the absence of an open licence (eg Creative Commons), permissions for further reuse of content should be sought from the publisher, author or other copyright holder.

Versions of research

The version in the Kent Academic Repository may differ from the final published version.

Users are advised to check <http://kar.kent.ac.uk> for the status of the paper. **Users should always cite the published version of record.**

Enquiries

For any further enquiries regarding the licence status of this document, please contact:

researchsupport@kent.ac.uk

If you believe this document infringes copyright then please contact the KAR admin team with the take-down information provided at <http://kar.kent.ac.uk/contact.html>

New Compact Star Cluster Candidates in the Galactic Plane

D. Froebrich^{1*}

¹ *Centre for Astrophysics and Planetary Science, University of Kent, Canterbury, CT2 7NH, UK*

Received sooner; accepted later

ABSTRACT

The sample of known star clusters, the fundamental building blocks of galaxies, in the Milky Way is still extremely incomplete for objects beyond a distance of 1–2 kpc. Many of the more distant and young clusters are compact and hidden behind large amounts of extinction. We thus utilised the deep high resolution near infrared surveys UGPS and VVV to uncover so far unknown compact clusters and to analyse their properties.

Images of all objects in the area covered by these two surveys, and which are listed as Galaxy in SIMBAD have been inspected and 125 so far unknown stellar clusters and candidate clusters have been identified. Based on the frequent associations with star formation indicators (nebulosities, IRAS sources, HII regions, masers) we find that the typical cluster in our sample is young, at distances between 1–10 kpc and has a typical apparent radius of 25". We suggest more systematic searches e.g. at all positions of 2MASS extended sources to increase the completeness of the known cluster sample beyond distances of 2 kpc.

Key words: Galaxy: open clusters and associations: general; galaxies: star clusters: general; Galaxy: evolution; Galaxy: general; Galaxy: structure

1 INTRODUCTION

The vast majority of stars form in clusters (Lada & Lada 2003), and most of these clusters dissolve on timescales of 10s of Myrs (Goodwin & Bastian 2006) to form the field star population. Thus, star clusters are the building blocks of galaxies and their study is intimately linked to understanding star formation and in particular the formation of more massive stars which are almost exclusively formed in clusters (Gvaramadze et al. 2012), with potential exceptions such as discussed e.g. in Oey et al. (2013).

Establishing large and complete cluster samples is vital if we for example want to understand the details of the cluster destruction/dissolution processes. In particular the study of the impact of tidal forces from the galactic potential, requires well characterised and bias free samples of clusters at a range of galactocentric radii. The current most complete lists of clusters and their properties contain a few thousand objects (e.g. about 2200 in the up to date online version¹ of Dias et al. (2002) and about 3000 in Kharchenko et al. (2013), plus a few hundred more in the additions by Schmeja et al. (2014) and Scholz et al. (2015). The latter paper also finds that our sample of known clusters is only complete to a distance of 1.8 kpc from the Sun, with still many old clusters missing at even shorter distances (Schmeja et al. 2014) and basically no clusters are known at distances further away than 5 kpc - see Fig. 7 in Schmeja et al. (2014). Kharchenko et al. (2013) also show that the projected surface number density of clusters at the position of the Sun is about

130 clusters per square kiloparsec in the disk. This implies that there should be of the order of $2-3 \times 10^4$ clusters in the Milky Way. Hence, only about 10 % of all clusters are currently catalogued and an even smaller fraction has its parameters determined accurately.

Many of the more distant undiscovered clusters are young and thus potentially associated with large amounts of extinction and projected against the Galactic plane. Furthermore, with typical sizes of about one parsec, these clusters will be of an apparent angular size of less than one arcminute for distances of about 3 kpc or higher. Hence, to discover and potentially analyse clusters missing in our current sample, deep high resolution infrared surveys are going to be of importance. Extensive searches in 2MASS (Skrutskie et al. 2006) have already uncovered a huge new population of new clusters and candidates (e.g. Dutra et al. (2003), Bica et al. (2003), Froebrich et al. (2007), Glushkova et al. (2010)). But the new deeper and higher resolution surveys such as UGPS (Lucas et al. 2008) and VISTA VVV (Minniti et al. 2010) will be able to uncover so far unrecognised objects which are more compact and fainter. Some searches for new clusters in these surveys have already been done (e.g. Solin et al. (2012), Borissova et al. (2011), Lucas et al. (2017) in prep.). However, many compact objects might have been overlooked. We thus aim to search these surveys at the positions of known extended, but potentially miss-classified objects and characterise them.

Our paper is structured as follows: The target selection and data analysis procedures are explained in Sect. 2. We present the newly discovered clusters and cluster candidates and their properties in Sect. 3.

* E-mail: df@star.kent.ac.uk

¹ <http://www.wilton.unifei.edu.br/ocdb/>

2 DATA ANALYSIS

2.1 Target Selection

The fact that a large fraction clusters at distances above about 2 kpc has not yet been discovered, is to some extent, but not entirely due to extinction in the Galactic plane and the large number of foreground and background stars in low latitude fields. One additional problem is spatial resolution. Assuming a typical cluster size of 0.5 pc, then at 5 kpc the cluster would appear only to have an extend of $20''$. Thus, even if there are many bright, detectable members, typical surveys such as 2MASS are not able to resolve all of the stars into individual point sources and the cluster will only be detected as an extended object instead. This is in particular true for young, embedded clusters which are typically also surrounded by reflection/emission nebulae. As young clusters constitute the majority of all clusters in the Galaxy (e.g. Lada & Lada (2003), Buckner & Froeblich (2014)), a large fraction of them might be detectable even in 2MASS but only as extended sources, which in many cases might have been classified (wrongly) as potential galaxies.

Hence, in order to identify potentially miss-classified star clusters, we used the SIMBAD² database. We extracted all objects from SIMBAD that were listed as Galaxy (`otype = 'G'`). We planed to analyse the NIR data from the deep high resolution UGPS and VISTA VVV surveys for these objects to establish their true nature. Thus, we limited the selection to objects with a K -band detection (i.e. $K_{\text{mag}} < 20.0$) in SIMBAD. This ensures we do not select extended objects only detected at mid or far-infrared wavelengths, but most likely sources with even an extended 2MASS source counterpart. Note that the limiting magnitude for extended sources in 2MASS is about $K = 14$ mag (Jarrett et al. 2000).

We also limited the search in SIMBAD to regions overlapping the UGPS and VVV survey fields. The borders of the surveys where chosen as listed below. Please note that the UGPS has its images orientated along the RA/DEC coordinates, while the VVV data has an image orientation along the Galactic coordinate system. Thus, the applied restrictions for UGPS (especially in latitude) are not the exact survey limits.

- For UGPS: $|b| < 2^\circ$ and $359^\circ < l < 15^\circ$
- For UGPS: $|b| < 5^\circ$ and $15^\circ < l < 107^\circ$
- For UGPS: $|b| < 5^\circ$ and $141^\circ < l < 230^\circ$
- For VVV: $|b| < 2^\circ$ and $295^\circ < l < 350^\circ$ (disk)
- For VVV: $-10^\circ < b < 5^\circ$ and $350^\circ < l < 10^\circ$ (bulge)

Thus, our selection covers a total area that we searched for potential miss-identified star clusters of about 1874 square degrees in UGPS and 520 square degrees in VVV. There is some overlap of 44 square degrees between UGPS and VVV near the Galactic Centre, where both surveys have available data. Thus, the total area surveyed is 2350 square degrees.

In total we find 4387 objects which pass our selection criteria, i.e. are listed as Galaxy in SIMBAD, have a detected K -band counterpart of at least 20th magnitude and are within the UGPS or VVV footprint.

2.2 NIR data

To investigate the high resolution UGPS and VVV images of the above selected 4387 objects in detail we have used the WSA³ and VSA⁴ databases to extract $JHK(s)$ images for each target. We extracted image cutouts with a size of $3' \times 3'$ around each object. For some targets no images or not all three images were available. This can be caused by the object either being close to the survey boundary (which is not straight) or some images are not (yet) included in the latest available data release due to not passing quality thresholds. Note that we used DR10 of the UGPS and DR4 for the VVV data.

In total 3409 (77.7%) of our targets have all three NIR images available in either UGPS or VVV. We have combined these images into $JHK(s)$ colour composites and visually inspected all of them to select all objects that could be real star clusters. For each target the colour composite images have been looked at in various zoom levels as well as different contrast settings to ensure all potential star clusters can be identified.

2.3 Star Cluster Identification

From all the JHK images we selected every object that visually could either be identified as a group or cluster of stars or a nebulous young stellar object. In other words we removed all the obvious galaxies from the target list. An investigation of the properties of all these galaxies as well as potential new galaxy clusters is planned, but outside the scope of this paper. Other objects we removed were clearly associated with extended emission from edges of HII regions and not stellar clusters. We also removed double entries, i.e. objects that had two entries as Galaxy in SIMBAD very close to each other, in the same cluster. Finally, all remaining objects were checked if they have an entry as a known star cluster in SIMBAD.

The above process resulted in the following:

- There are 125 candidates for so far unknown/unpublished groups or clusters of (mostly) young stars;
- There are 19 objects that are known cluster candidates; There are 84 known star clusters which are not analysed any further in this paper;
- There is one object that cannot be reliably identified as either a star cluster candidate or background galaxy (see discussion below).

Images of all the new star cluster candidate objects have been inspected a second time in detail to determine some of the cluster properties. We manually estimated the central position of the cluster, as well as its apparent radius (R_{Cl}) and also approximately counted manually the apparent number of stars visible in the NIR images that seem to belong to the cluster.

Based on this inspection, we further divided the sample of 125 objects into clear cluster candidates (star clusters, hereafter), with an obvious overdensity of NIR detectable stars and less clear cluster candidate objects (candidate clusters hereafter). The latter mostly encompasses very nebulous objects and small/less populous groups of young stars. This split has resulted in 77 new clusters and 48 cluster candidates. Similarly to the new clusters, we also classified the 19 known cluster candidates. In total 16 of these we judge to be clusters, the remaining 3 fall into the candidate cluster category.

Finally, all the 125 candidate objects, as well as the 19 known

² <http://simbad.u-strasbg.fr/simbad/>

³ <http://wsa.roe.ac.uk/index.html>

⁴ <http://horus.roe.ac.uk/vsa/index.html>

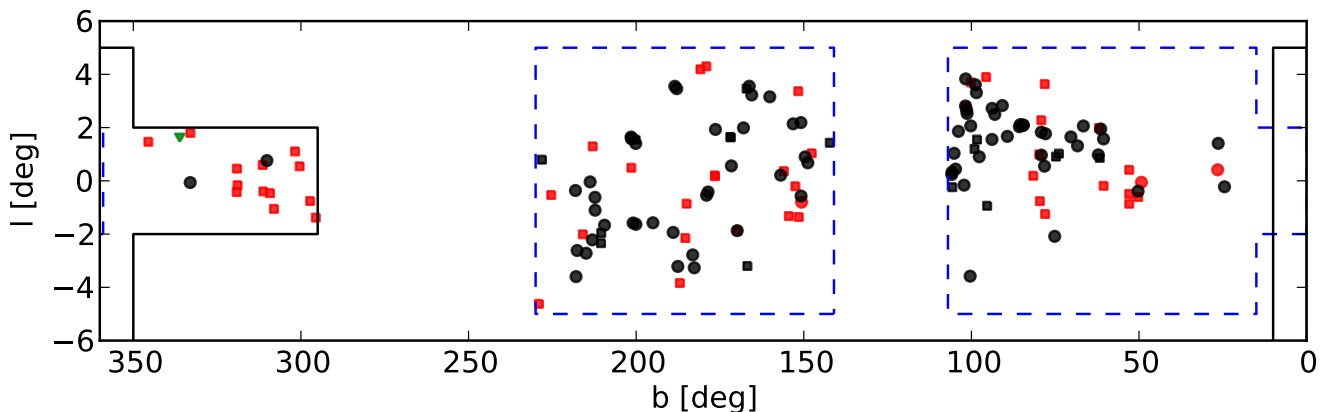


Figure 1. Distribution along the Galactic plane of all new clusters and candidate objects. The symbols indicate the following: black circles - new clusters; black square - confirmed clusters; red circle - new cluster candidates; red squares - confirmed cluster candidates; green triangle - unknown object; The area outlined by the black solid line indicated the VVV survey coverage, the area outlined by the blue dashed line indicates the UGPS coverage.

cluster candidates have been checked if they are associated with an HII region or a maser, and if the NIR images show a detectable nebulosity. We also cross-matched all objects with IRAS and MSX sources and in particular objects in the Red MSX Source (RMS) survey (Lumsden et al. 2013) database⁵. The latter objects have in most cases a known distance determined from radial velocities (Urquhart et al. 2014), which we have extracted. We list all the properties of the objects in Table A1 in the Appendix. Note that of the 125 candidate objects 26 have been previously discovered in UGPS data by an alternative search method, and will be published in Lucas et al. (2017, in prep.). These are 24 of our 77 new clusters and 2 of our 48 new cluster candidates. We refrain from listing the properties of these objects in Table A1 and also do not show their images in Tables B1 and B2 as they will be presented in Lucas et al. (2017, in prep.). They are, however, included in our general analysis of their properties in Sect. 3 and are shown in Fig. 1.

2.4 Photometry and Cluster Membership

To investigate the cluster candidates and their members in more detail, we have downloaded the full point source catalogues within 5' of each object from the WSA and VSA databases. We extract the $JHK(s)$ magnitudes (using `AperMag3`) as well as the `pstar` parameter for each star and only include stars with `pstar` > 0.9 and detections in all three filters in our subsequent analysis. See Lucas et al. (2008) and Minniti et al. (2010) for a detailed descriptions of how the magnitudes are measured and the `pstar` value for each star is determined.

For each cluster candidate we calculate the number of additional stars (N_{Cl}) within R_{Cl} compared to the surrounding area (outside R_{Cl} , within 5'). This number gives a measure of how significant an overdensity of stars the cluster represents compared to the surrounding field i.e. estimates the number of NIR detectable cluster members with reliable photometry. In regions of extended large dark clouds and increased extinction these estimates can of course be erroneous. Furthermore, even in these high resolution surveys, many stars are not resolved and thus will not have a sufficiently accurate brightness measurement to be included in the analysis. Especially in young and very embedded clusters, which make

up a large fraction of our objects (see below), many stars are not detected at the shorter (J -band) wavelengths. Thus, some clusters even show a negative number of members compared to the background population despite a clear cluster being visible in the K -band images (e.g. Cl 019, Cl 043 and in particular Cl 062).

We also investigated NIR colour-magnitude ($J-K$ vs. K) diagrams (CMDs) and colour-colour ($H-K$ vs $J-H$) diagrams (CCDs) of stars in the cluster area compared to the control field around them. However, due to the limited photometry available, and the generally small number of stars, it has been proven impossible to use well established photometric decontamination techniques (e.g. following Bonatto & Bica (2007), Froebrich et al. (2010) or Buckner & Froebrich (2014)) to reliably identify the most likely cluster members in order to fit isochrones to these diagrams. As there is basically nothing to be gained from these diagrams we refrain from showing them. It might be possible with careful psf-photometry of the UGPS/VVV images to improve the photometry, but this is beyond the scope of this paper.

3 RESULTS AND DISCUSSION

3.1 Distribution of New Clusters and Candidates

In total we have identified 77 new clusters, 53 of which are not included in the list of Lucas et al. (2017, in prep.). The images of these clusters are shown in Table B1 in Appendix B and all the determined properties are listed in Table A1. We also identify 48 objects as candidate clusters or groups of stars, 46 of which are not included in the list of Lucas et al. (2017, in prep.). The images of these candidates are also shown in Table B2 in Appendix B and all the properties are listed in Table A1.

We show the general distribution along the Galactic plane of all the newly discovered objects in Fig. 1. The figure shows that most of the newly discovered clusters are away from the Galactic Centre. Only two of the new clusters are in the area covered by VVV, the remainder are in the UGPS area. This can to some extent be attributed to the density of SIMBAD objects classified as Galaxy in the different fields. While the disk part of VVV has 0.6 'G' type objects per square degree, the equivalent UGPS field has 1.0 such objects per square degree and the UGPS field in the outer Galaxy

⁵ http://rms.leeds.ac.uk/cgi-bin/public/RMS_DATABASE.cgi has 3.4 objects per square degree. The latter is certainly caused

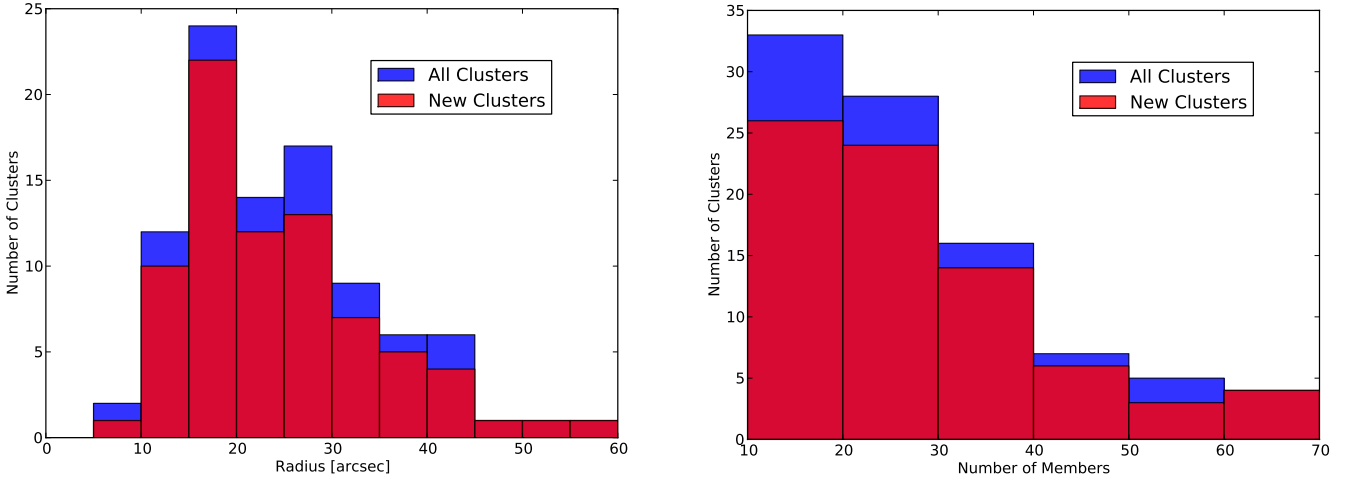


Figure 2. Distribution of the apparent radii (left panel) and number of manually detected cluster members (right panel) of the clusters discovered in our sample. The red histogram represents the newly discovered clusters, while the blue histogram also includes the new clusters identified amongst the known cluster candidates. Both histograms include all objects, including the ones that are included in the list from Lucas et al. (2017, in prep.).

by the lower extinction and thus many more real galaxies in the sample. The differences between the two UGPS and VVV inner disk fields are very minor when considering the actual extend. The number of new clusters and candidates found in the equivalent area of the inner disk in UGPS is almost identical to the number found in the VVV area. Hence, most of the new clusters are found more than 60 degrees away from the Galactic Centre.

Amongst the known cluster candidates in our list (most are from Solin et al. (2012), one from Ivanov et al. (2005) and one from Camargo et al. (2015)), we identify 16 as real clusters. In case of the remaining 3 objects no clear verdict can be reached from our data. Thus, these objects remain cluster candidates. All their images are shown in Table B3 in Appendix B and all the properties are listed in Table A1. In particular object CI 142, known as Camargo 442 (Camargo et al. 2015), seems not to be a real cluster. Instead the *JHK* images suggest that this is just extended nebulosity surrounding a single star and not a cluster.

One of our objects (CI 145) is of an unclear nature (see Fig. B4 in Appendix B). It is situated in a very crowded field near the Galactic Centre. A detailed inspection of the *JHK* image seems to suggest an increased number of fainter stars towards the centre as well as nebulosity. On the other hand, it is not clearly identifiable as a background galaxy. The 2MASS images of the globular cluster FSR 1735 (Froebrich et al. 2007) appear somehow similar to this object, hence there is still a possibility that this is a compact, distance rich cluster and not a background galaxy.

3.2 Properties of New Clusters and Candidates

The properties of all new clusters, new cluster candidates and known candidates in our sample are summarised in Table A1. The table is organised by object group (new clusters, new candidates, etc.) and lists the object identifier, the coordinates (J2000 and galactic), the cross identification IDs from IRAS and MSX, associations with known HII regions, masers and nebulosities (identified in the *JHK* images), the distances obtained from associated RMS sources, the apparent radii as well as the number of potential members determined manually from the images and automatically from the photometric catalogues.

Of all our objects, 88.3% have an association with an IRAS

source. This percentage is basically identical for the new clusters and the new cluster candidates. Similarly, 25.5% of all objects are associated with an MSX source with identical percentages for the different groups.

The fraction of objects that are associated with star formation indicators such as HII regions and masers are also investigated. In total 27.6% of objects are associated with HII regions and 10.3% with masers. There are slight differences in the percentages between the new clusters and the new candidates. While about 1/3 of the new clusters are associated with HII regions, only 1/5 of the new cluster candidates have such an association. This could be due to the fact the HII regions are indicators of slightly more massive and evolved stars, thus increasing the likelihood of detecting more stars in the *JHK* images and thus their classification as a new cluster. We find that 1/10 of the new clusters and 1/6 of the new cluster candidates have associations with known masers. As masers are indicators of more embedded younger massive protostars, it is understandable that due to the increased extinction and younger age of these objects it is more difficult to identify a sufficient number of members in the *JHK* images to classify the objects as new clusters.

In total 77.9% of all objects are associated with detectable nebulous NIR emission. Again, there is some variation of this fraction between the new clusters (74.0%) and the new cluster candidates (87.5%). Similarly to the association with HII regions and masers, this difference can be explained by extinction. Increased amounts of dust tend to lead to more detectable nebulosity and at the same time decreased detectability of cluster members and thus, more likely a classification of an object as cluster candidate.

We show the distribution of apparent radii measured for all clusters (known candidates and new clusters) in the left panel of Fig. 2. Most clusters have apparent radii between 10'' and 45'' with a wide distribution. The median radius of the distribution is 23''. Thus, all the clusters are quite compact, caused by the selection of the objects as miss-classified galaxies. Objects much more extended than this would most likely have been classified correctly as clusters even with lower resolution 2MASS data. For comparison, the MWSC list by Kharchenko et al. (2013), including the additions by Schmeja et al. (2014) and Scholz et al. (2015), does only contain very few objects with a core radius of less than 36'', and

no objects at all with an apparent radius smaller than $60''$. Given the large number of compact clusters identified in this work, compared to the small number of known objects in the current up to date literature shows the potential for future discoveries in these high resolution infrared surveys.

We display the distribution of the manually estimated cluster members for all clusters (known candidates and new clusters) in the right panel of Fig. 2. As to be expected there are significantly more clusters with a smaller number of members. The median number of manually detected members is 23 stars. The distribution of automatically detected members in the clusters looks similar, just with a smaller number of clusters in each bin. This is caused, as explained in Sect. 2.4, by the fact that in regions with increased extinction the automatic determination of the number of members fails, as background stars to the cluster are not detected in the cluster field.

As can be seen in Table A1, the range of distances for the clusters with associations to RMS objects is very large. The distances range from just above 1 kpc to slightly more than 10 kpc, with a median value of about 6 kpc. These clusters are hence typically much further away than the objects listed in the MWSC list, which have typical distances of 1.5–2.5 kpc. The typical distances combined with the median apparent radius of the clusters, lead to a typical radius of 0.7 pc for the clusters in our sample. However, only a fraction of 18 % of the new clusters have a distance estimate. One could try to fit isochrones to potential cluster members in order to obtain further distance estimates for the remainder of the sample. However, as discussed in Sect. 2.4, it has proven not possible to do with the currently available pipeline aperture photometry from UGPS/VVV. This is mostly caused by the compactness of the new clusters and the in part high extinction, which prevents detection and/or reliable photometry in the J -band.

4 CONCLUSIONS

In order to identify potentially undetected star cluster (candidates) in the Galactic plane, we manually inspected images from the UGPS and VVV surveys for all objects classified as ‘Galaxy’ in SIMBAD to identify miss-classified star clusters. A total of 4387 objects were initially selected and JHK images for 3409 of those where available and investigated in detail in an area of 2350 square degrees over both surveys.

Amongst the investigated objects we identified 125 so far unknown cluster candidates, 19 known cluster candidates and 1 object of unclear nature. We performed a detailed inspection of the so far unknown objects and identified 77 new clusters and 48 cluster candidates. All but three of the already known cluster candidates can be confirmed as clusters with the utilised higher resolution UGPS and VVV data.

A large fraction of the newly identified clusters and candidates are associated with star formation indicators. Overall, about 80 % have detectable NIR nebulosities, about 90 % are associated with IRAS sources, 25 % with MSX sources and HII regions and 10 % with masers. We extracted the distances of the associated MSX sources and find that they range from 1 to 10 kpc, with a median of about 6 kpc. The typical apparent radius of the new clusters is about $25''$ corresponding to about 0.7 pc at the typical distance. Thus, our newly identified clusters are young, apparently compact clusters at distances of several kiloparsec. Detailed cluster member identification and isochrone fitting for the new objects cannot be performed as the currently available photometry is not of sufficient quality due to the compactness of the detected clusters. PSF

photometry of the original survey data might in future allow such investigations.

The large number of new clusters detected by our search is promising for future work. While the discovered objects are in no way numerous enough to account for the incompleteness in our cluster samples beyond about 1–2 kpc, they show that many of these missing clusters can be discovered in the available datasets. A more systematic search in UGPS/VVV, e.g. at all positions of extended 2MASS sources or near groups of UGPS/VVV objects with low p_{star} values, should reveal a substantial number of so far uncatalogued clusters.

ACKNOWLEDGEMENTS

The author would like to thank J. Urquhart for providing the RMS based distances reported in the paper. He also acknowledges the comments on some of the sources provided by D. Minniti, P.W. Lucas and T. Gledhill.

REFERENCES

- Bica E., Dutra C. M., Soares J., Barbuy B., 2003, *A&A*, 404, 223
 Bonatto C., Bica E., 2007, *MNRAS*, 377, 1301
 Borissova J., Bonatto C., Kurtev R., Clarke J. R. A., Peñaloza F., Sale S. E., Minniti D., et al., 2011, *A&A*, 532, A131
 Buckner A. S. M., Froebrich D., 2014, *MNRAS*, 444, 290
 Camargo D., Bonatto C., Bica E., 2015, *MNRAS*, 450, 4150
 Dias W. S., Alessi B. S., Moitinho A., Lépine J. R. D., 2002, *A&A*, 389, 871
 Dutra C. M., Bica E., Soares J., Barbuy B., 2003, *A&A*, 400, 533
 Froebrich D., Schmeja S., Samuel D., Lucas P. W., 2010, *MNRAS*, 409, 1281
 Froebrich D., Scholz A., Raftery C. L., 2007, *MNRAS*, 374, 399
 Glushkova E. V., Kuposov S. E., Zolotukhin I. Y., Beletsky Y. V., Vlasov A. D., Leonova S. I., 2010, *Astronomy Letters*, 36, 75
 Goodwin S. P., Bastian N., 2006, *MNRAS*, 373, 752
 Gvaramadze V. V., Weidner C., Kroupa P., Pflamm-Altenburg J., 2012, *MNRAS*, 424, 3037
 Ivanov V. D., Borissova J., Bresolin F., Pessev P., 2005, *A&A*, 435, 107
 Jarrett T. H., Chester T., Cutri R., Schneider S., Skrutskie M., Huchra J. P., 2000, *AJ*, 119, 2498
 Kharchenko N. V., Piskunov A. E., Schilbach E., Röser S., Scholz R.-D., 2013, *A&A*, 558, A53
 Kumar M. S. N., Ojha D. K., Davis C. J., 2003, *ApJ*, 598, 1107
 Lada C. J., Lada E. A., 2003, *ARA&A*, 41, 57
 Lucas P. W., Hoare M. G., Longmore A., Schröder A. C., Davis C. J., Adamson A., Bandyopadhyay R. M., et al. 2008, *MNRAS*, 391, 136
 Lumsden S. L., Hoare M. G., Urquhart J. S., Oudmaijer R. D., Davies B., Mottram J. C., Cooper H. D. B., Moore T. J. T., 2013, *ApJS*, 208, 11
 Minniti D., Lucas P. W., Emerson J. P., Saito R. K., Hempel M., Pietrukowicz P., Ahumada A. V., Alonso M. V., Alonso-García J., Arias J. I., Bandyopadhyay R. M., 2010, *New Astronomy*, 15, 433
 Oey M. S., Lamb J. B., Kushner C. T., Pellegrini E. W., Graus A. S., 2013, *ApJ*, 768, 66
 Schmeja S., Kharchenko N. V., Piskunov A. E., Röser S., Schilbach E., Froebrich D., Scholz R.-D., 2014, *A&A*, 568, A51

6 *Froeblich, D.*

Scholz R.-D., Kharchenko N. V., Piskunov A. E., Röser S., Schilbach E., 2015, *A&A*, 581, A39

Skrutskie M. F., Cutri R. M., Stiening R., Weinberg M. D., Schneider S., Carpenter J. M., Beichman C., Capps R., 2006, *AJ*, 131, 1163

Solin O., Ukkonen E., Haikala L., 2012, *A&A*, 542, A3

Urquhart J. S., Figura C. C., Moore T. J. T., Hoare M. G., Lumsden S. L., Mottram J. C., Thompson M. A., Oudmaijer R. D., 2014, *MNRAS*, 437, 1791

APPENDIX A: CLUSTER DATA TABLE

Table A1: This table lists the properties of all clusters and candidates that are not included in the list of Lucas et al. (2017, in prep). The table is organised by object group (new clusters, new candidates, etc.) and lists the object identifier, the coordinates (J2000 and galactic), the cross identification IDs from IRAS and MSX, associations with known HII regions, masers and nebulosities (identified in the *JHK* images), the distances obtained from associated RMS sources, the apparent radii as well as the number of potential members determined manually from the images and automatically from the photometric catalogues.

Name	Coordinates				Cross-ID		Association with			Distance [kpc]	Radius [arcsec]	Number of Stars	
	RA/DEC (J2000) [h:m:s]	[°:′:″]	Galactic (l,b) [deg]		IRAS	MSX	HII	Maser	Nebula			Man.	Aut.
New Clusters													
CI001	04:01:26.4	+53:43:17	148.799412	+0.677165	IRAS 03575+5334	–	N	N	N	–	18	30	11
CI002	04:05:56.6	+51:27:05	150.814877	–0.571217	–	–	N	N	Y	–	15	10	–
CI003	04:06:25.5	+53:21:49	149.591151	+0.900032	IRAS 04025+5313	–	N	N	Y	–	26	40	4
CI004	04:18:32.6	+53:26:03	150.859922	+2.188007	IRAS 04146+5318	G150.8602+02.1879	Y/N	Y	N	–	32	50	24
CI005	04:29:00.1	+51:45:23	153.171059	+2.140904	IRAS 04251+5138	–	Y	N	Y	–	28	15	21
CI006	04:35:58.9	+47:43:03	156.895187	+0.212232	IRAS 04322+4736	–	N	N	N	–	20	30	5
CI007	05:01:39.7	+47:07:22	160.144438	+3.155929	IRAS 04579+4703	G160.1452+03.1559	Y	N	Y	1.94	27	40	–
CI013	05:39:28.4	+24:56:30	182.678494	–3.265738	IRAS 05363+2454	–	Y	Y	N	–	10	15	4
CI014	05:40:29.6	+29:56:48	178.553723	–0.418188	IRAS 05372+2955	–	N	N	N	–	16	10	3
CI015	05:41:05.2	+29:30:26	178.994673	–0.541804	IRAS 05378+2928	–	N	N	Y	–	25	25	12
CI016	05:42:20.6	+24:48:36	183.134536	–2.782362	IRAS 05393+2447	–	N	N	N	–	29	35	17
CI017	05:44:23.9	+33:03:51	176.341522	+1.931052	IRAS 05411+3302	–	N	N	Y	–	56	30	25
CI018	05:50:40.1	+20:48:10	187.562049	–3.214981	IRAS 05476+2047	–	N	N	N	–	26	15	14
CI019	05:58:24.5	+20:13:57	188.969785	–1.937577	IRAS 05554+2013	G188.9696–01.9380	N	N	Y	2.0	30	25	–
CI020	06:12:06.9	+15:09:04	195.000702	–1.575500	–	–	N	N	Y	–	19	15	–
CI021	06:16:31.8	+23:47:23	187.902651	+3.461314	IRAS 06134+2348	–	N	N	Y	–	15	30	6
CI022	06:18:04.2	+23:19:14	188.483899	+3.551225	IRAS 06150+2320	–	N	N	Y	–	20	50	11
CI023	06:21:47.7	+10:39:23	200.078150	–1.632706	IRAS 06190+1040	G200.0789–01.6323	Y	N	N	5.78	40	70	20
CI024	06:23:34.3	+09:56:19	200.917363	–1.583128	IRAS 06208+0957	G200.9166–01.5827	Y/N	N	Y	5.54	34	40	10
CI025	06:32:51.3	+12:01:34	200.127573	+1.404202	IRAS 06300+1203	–	N	N	N	–	19	30	6
CI026	06:35:50.0	+10:59:49	201.377469	+1.578306	–	–	N	N	N	–	16	15	6
CI027	06:35:56.1	+11:00:19	201.381527	+1.604296	IRAS 06331+1102	–	N	N	Y	–	27	20	6
CI028	06:36:19.3	+10:54:26	201.512264	+1.643583	IRAS 06335+1057	–	N	N	N	–	17	30	15
CI038	13:51:59.6	–61:15:39	310.146375	+0.759752	IRAS 13484–6100	–	N	Y	Y	–	30	20	–
CI039	16:18:57.4	–50:23:59	333.029624	+0.065123	–	–	N	Y	Y	–	26	20	–
CI041	18:36:47.1	–07:35:41	24.507573	+0.223496	IRAS 18340–0738	–	Y	N	Y	–	13	20	–
CI044	19:39:32.7	+26:05:25	61.422407	+1.947718	IRAS 19374+2558	–	N	N	Y	–	17	20	–
CI046	19:50:53.0	+30:38:10	66.608918	+2.060751	IRAS 19489+3030	–	N	N	Y	–	13	10	–
CI047	19:58:03.1	+31:44:07	68.341812	+1.313669	IRAS 19560+3135	G068.3418+01.3138	Y	N	Y	11.66	12	10	–
CI048	20:01:37.4	+33:35:28	70.316479	+1.648899	IRAS 19597+3327	G070.3164+01.6493	Y/N	N	Y	7.42	17	20	–
CI049	20:21:55.1	+39:59:46	77.900648	+1.767362	–	G077.8999+01.7678	Y	N	Y	1.4	23	10	–

Continued on next page

Table A1 – continued from previous page

Name	Coordinates				Cross-ID		Association with			Distance [kpc]	Radius [arcsec]	Number of Stars	
	RA/DEC (J2000) [h:m:s]	[°:':"]	Galactic (l,b) [deg]		IRAS	MSX	HII	Maser	Nebula			Man.	Aut.
Cl050	20:25:25.3	+41:03:19	79.150728	+1.829256	IRAS 20236+4053	–	N	N	Y	–	15	20	–
Cl051	20:27:58.8	+39:32:09	78.196161	+0.550244	IRAS 20261+3922	G078.1952+00.5497	Y/N	N	Y	8.51	9	10	1
Cl053	20:29:46.8	+35:31:42	75.154768	–2.084232	IRAS 20278+3521	–	N	Y	Y	–	24	30	–
Cl054	20:41:53.5	+45:32:00	84.534232	+2.089183	IRAS 20402+4521	–	N	N	Y	–	14	25	–
Cl055	20:41:55.2	+45:32:39	84.545836	+2.091922	–	–	N	N	Y	–	12	15	–
Cl056	20:44:53.1	+46:14:15	85.410346	+2.114474	IRAS 20431+4603	–	N	N	Y	–	13	15	–
Cl057	20:46:17.2	+46:24:35	85.695990	+2.032407	IRAS 20446+4613	–	Y	N	Y	–	38	20	–
Cl058	21:01:34.9	+48:55:01	89.272880	+1.670386	IRAS 20599+4843	G089.2727+01.6703	Y	N	Y	8.06	23	30	–
Cl059	21:02:21.8	+50:48:35	90.777103	+2.827686	IRAS 21007+5036	G090.7764+02.8281	Y	N	Y	1.74	15	10	–
Cl060	21:13:38.9	+52:14:01	93.014939	+2.495089	IRAS 21120+5201	G093.0166+02.4953	Y	N	N	–	19	10	–
Cl061	21:16:19.3	+52:58:57	93.837221	+2.720457	IRAS 21147+5246	–	N	N	N	–	16	20	2
Cl062	21:21:53.6	+52:10:47	93.859904	+1.554173	IRAS 21202+5157	G093.8588+01.5551	Y	N	Y	6.36	33	70	–
Cl063	21:36:46.0	+56:38:56	98.506636	+3.311011	IRAS 21351+5625	–	N	N	Y	–	17	20	13
Cl064	21:37:04.4	+57:05:16	98.832037	+3.609138	–	–	N	N	N	–	19	20	–
Cl066	21:52:02.2	+56:47:49	100.197892	+2.064316	IRAS 21503+5633	G100.1974+02.0643	Y/N	N	Y	5.85	29	40	–
Cl067	21:52:30.6	+59:06:52	101.703900	+3.828645	IRAS 21509+5852	–	N	N	N	–	16	20	2
Cl068	21:56:15.1	+57:50:42	101.296341	+2.530582	IRAS 21545+5736	–	N	N	Y	–	23	15	–
Cl069	21:56:27.3	+58:01:50	101.432089	+2.660077	IRAS 21548+5747	–	Y	N	Y	–	39	70	27
Cl070	21:57:44.6	+58:21:06	101.763679	+2.809178	IRAS 21561+5806	G101.7639+02.8100	Y/N	Y	Y	7.81	32	25	–
Cl071	22:13:16.6	+56:12:14	102.192782	–0.162377	IRAS 22114+5557	–	N	N	Y	–	13	15	–
Cl072	22:15:08.7	+58:49:16	103.875995	+1.857624	IRAS 22134+5834	G103.8744+01.8558	Y	N	Y	1.59	49	20	17
Cl075	22:26:57.4	+58:49:41	105.163562	+1.033268	IRAS 22251+5834	–	N	N	Y	–	14	10	–
New Cluster Candidates													
Cl078	03:56:57.8	+54:45:02	147.633127	+1.033568	IRAS 03530+5436	–	N	N	N	–	–	–	–
Cl079	04:05:47.0	+50:25:04	151.486411	–1.357451	IRAS 04020+5017	–	N	N	N	–	–	–	–
Cl080	04:19:10.7	+48:24:57	154.445183	–1.325439	IRAS 04154+4817	–	N	N	Y	–	–	–	–
Cl081	04:27:49.6	+53:43:08	151.627347	+3.367920	IRAS 04238+5336	–	N	N	Y	–	–	–	–
Cl082	04:32:44.6	+48:31:49	155.931246	+0.365437	IRAS 04290+4825	–	N	N	Y	–	–	–	–
Cl083	04:15:22.0	+50:34:36	152.496404	–0.205135	IRAS 04115+5027	–	N	N	Y	–	–	–	–
Cl084	05:11:22.8	+36:21:20	169.835550	–1.878073	IRAS 05081+3616	–	N	N	N	–	–	–	–
Cl085	05:37:42.0	+32:00:48	176.486090	+0.177157	–	–	N	N	N	–	–	–	–
Cl086	05:37:50.8	+32:00:40	176.504622	+0.202220	–	–	N	N	N	–	–	–	–
Cl087	05:47:04.3	+20:59:41	186.965545	–3.837873	–	–	N	N	Y	–	–	–	–
Cl088	05:49:39.7	+23:16:59	185.308898	–2.146923	IRAS 05466+2316	–	N	Y	Y	–	–	–	–
Cl089	05:53:43.6	+24:14:45	184.954832	–0.855921	IRAS 05506+2414	G184.9551–00.8559	N	N	Y	3.66	–	–	–
Cl090	06:00:33.4	+31:56:44	179.037040	+4.299981	IRAS 05573+3156	G179.0380+04.3003	N	N	Y	1.1	–	–	–
Cl091	06:04:10.1	+30:20:24	180.820245	+4.188061	IRAS 06009+3020	–	N	N	Y	–	–	–	–
Cl092	06:31:58.7	+10:27:48	201.414795	+0.492048	IRAS 06292+1029	–	N	N	Y	–	–	–	–

Continued on next page

Table A1 – continued from previous page

Name	Coordinates				Cross-ID		Association with			Distance [kpc]	Radius [arcsec]	Number of Stars	
	RA/DEC (J2000) [h:m:s]	[°:′:″]	Galactic (l,b) [deg]		IRAS	MSX	HII	Maser	Nebula			Man.	Aut.
CI 093	06:49:40.2	−03:32:52	215.889431	−2.009736	IRAS 06471−0329	–	N	N	Y	–	–	–	–
CI 095	07:04:21.6	−16:23:20	228.993299	−4.619786	IRAS 07020−1618	–	N	N	Y	–	–	–	–
CI 096	07:12:24.5	−11:15:34	225.326623	−0.531525	IRAS 07100−1110	–	Y	N	Y	–	–	–	–
CI 097	11:45:04.7	−63:17:46	295.558094	−1.378464	IRAS 11426−6301	–	N	N	Y	–	–	–	–
CI 098	12:00:57.0	−63:04:10	297.251695	−0.755942	IRAS 11583−6247	–	N	N	Y	–	–	–	–
CI 099	12:29:41.7	−62:13:09	300.401305	+0.545612	IRAS 12268−6156	–	N	N	Y	–	–	–	–
CI 100	12:41:17.6	−61:44:42	301.731465	+1.103014	IRAS 12383−6128	–	N	N	Y	–	–	–	–
CI 101	13:37:20.7	−63:28:12	308.031655	−1.053791	IRAS 13338−6312	–	N	N	Y	–	–	–	–
CI 102	13:46:37.0	−62:39:30	309.219610	+0.462208	IRAS 13431−6224	–	N	N	Y	–	–	–	–
CI 103	14:02:36.2	−61:05:45	311.425369	+0.596829	IRAS 13590−6051	–	Y	N	Y	–	–	–	–
CI 104	14:02:52.8	−62:07:23	311.177140	−0.400493	IRAS 13592−6153	–	N	N	Y	–	–	–	–
CI 105	14:59:29.2	−58:20:10	319.089385	+0.460397	IRAS 14556−5808	–	N	N	Y	–	–	–	–
CI 106	15:00:35.0	−58:58:10	318.915062	+0.164954	–	–	Y	Y	Y	–	–	–	–
CI 107	15:03:13.7	−59:04:29	319.163190	−0.420600	IRAS 14593−5852	–	Y	N	Y	–	–	–	–
CI 108	16:10:38.7	−49:05:59	332.955261	+1.802102	IRAS 16069−4858	–	Y	N	Y	–	–	–	–
CI 109	16:59:42.3	−40:03:45	345.494751	+1.466657	IRAS 16562−3959	–	N	Y	Y	–	–	–	–
CI 110	19:25:57.9	+15:03:02	50.222047	−0.606428	IRAS 19236+1456	G050.2213−00.6063	Y	N	Y	3.34	–	–	–
CI 111	19:27:34.8	+17:54:37	52.921318	+0.414364	IRAS 19253+1748	G052.9217+00.4142	N	Y	Y	5.06	–	–	–
CI 112	19:30:54.7	+17:28:44	52.922557	−0.488824	IRAS 19286+1722	G052.9221−00.4892	Y/N	N	Y	5.06	–	–	–
CI 113	19:32:16.1	+17:17:54	52.920171	−0.859438	IRAS 19300+1711	AGAL052.919−00.861	N	N	Y	–	–	–	–
CI 114	19:40:34.6	+26:34:15	61.954815	+1.982962	IRAS 19385+2627	–	N	N	Y	–	–	–	–
CI 115	19:45:52.5	+24:17:42	60.575275	−0.186735	IRAS 19437+2410	G060.5750−00.1861	Y	N	Y	7.48	–	–	–
CI 116	20:14:25.9	+41:13:37	78.123116	+3.633933	IRAS 20126+4104	G078.1224+03.6320	N	Y	Y	1.4	–	–	–
CI 117	20:23:23.9	+41:17:40	79.127561	+2.278287	IRAS 20216+4107	G079.1272+02.2782	Y	N	Y	1.4	–	–	–
CI 118	20:30:50.9	+41:02:30	79.736752	+0.990351	IRAS 20290+4052	–	N	Y	Y	–	–	–	–
CI 119	20:34:49.9	+38:19:07	78.001769	−1.243995	IRAS 20329+3808	–	N	N	Y	–	–	–	–
CI 121	20:39:58.0	+41:59:15	81.517594	+0.192362	–	G081.5168+00.1926	Y	N	Y	1.4	–	–	–
CI 122	21:18:52.8	+55:03:23	95.587783	+3.898574	IRAS 1173+5450	–	N	Y	Y	–	–	–	–
CI 123	21:44:04.8	+58:01:46	100.162064	+3.696814	IRAS 1425+5747	–	N	N	Y	–	–	–	–
CI 124	21:55:41.8	+57:58:31	101.318808	+2.678575	IRAS 1540+5744	G101.3193+02.6785	N	N	Y	6.24	–	–	–
CI 125	21:57:05.5	+58:17:54	101.663280	+2.819535	IRAS 1554+5803	–	N	N	N	–	–	–	–
Confirmed Cluster Candidates													
CI 126	03:27:31.4	+58:19:22	142.245218	+1.429872	IRAS 03235+5808	G142.2446+01.4299	Y/N	N	Y	4.15	31	50	9
CI 127	04:56:55.2	+37:57:17	166.813749	−3.198304	IRAS 04535+3752	G166.8141−03.1986	Y/N	N	Y	2.0	41	50	54
CI 128	05:25:40.6	+41:41:53	167.059948	+3.463957	IRAS 05221+4139	–	N	N	Y	–	42	40	13
CI 129	05:31:28.0	+36:43:01	171.835302	+1.644529	–	–	N	N	N	–	23	30	9
CI 130	05:31:28.7	+36:41:54	171.852162	+1.636293	–	–	N	N	N	–	19	20	5
CI 131	06:33:27.2	+12:03:31	200.166170	+1.549008	IRAS 06306+1205	–	N	N	Y	–	39	20	37

Continued on next page

Table A1 – continued from previous page

Name	Coordinates				Cross-ID		Association with			Distance [kpc]	Radius [arcsec]	Number of Stars	
	RA/DEC (J2000) [h:m:s]	[°:':"]	Galactic (l,b) [deg]		IRAS	MSX	HII	Maser	Nebula			Man.	Aut.
Cl 132	06:38:36.6	+01:07:20	210.469190	-2.341123	IRAS 06360+0109	–	N	N	N	–	16	15	–
Cl 133	06:39:52.2	+01:20:52	210.412543	-1.957914	IRAS 06372+0123	–	N	N	N	–	25	15	3
Cl 134	07:22:30.8	-13:05:26	228.099152	+0.796587	IRAS 07201-1259	–	N	N	Y	–	27	30	9
Cl 135	19:44:23.5	+25:48:42	61.720129	+0.863272	IRAS 19423+2541	G061.7201+00.8630	Y/N	N	Y	13.99	14	20	–
Cl 136	20:13:34.2	+36:15:00	73.877590	+1.024991	IRAS 20116+3605	G073.8775+01.0245	Y/N	N	Y	9.28	26	25	–
Cl 137	20:16:27.4	+36:54:54	74.752565	+0.912439	IRAS 20145+3645	G074.7541+00.9132	Y/N	N	Y	9.29	14	15	–
Cl 138	21:39:41.1	+51:20:36	95.298227	-0.937191	IRAS 21379+5106	–	N	Y	Y	–	21	15	9
Cl 139	21:44:03.1	+55:12:11	98.320050	+1.551357	IRAS 21423+5458	–	N	N	Y	–	9	10	–
Cl 140	21:49:40.5	+55:24:50	99.069107	+1.199380	IRAS 21479+5510	–	N	N	N	–	30	15	–
Cl 141	22:35:17.6	+57:59:53	105.677118	-0.238204	IRAS 22333+5744	–	N	N	Y	–	29	15	–
Unconfirmed Cluster Candidates													
Cl 142	04:04:13.4	+51:22:59	150.660242	-0.800726	IRAS 04004+5114	–	N	N	Y	–	–	–	–
Cl 143	18:38:16.1	-05:29:33	27.419567	+0.866342	IRAS 18355-0532	–	N	N	Y	–	–	–	–
Cl 144	19:22:07.8	+14:29:20	49.288593	-0.055411	IRAS 19198+1423	G049.2982-00.0582	N	N	Y	5.4	–	–	–
Unclassified Candidate Object													
Cl 145	16:24:49.9	-46:58:52	337.536565	+3.038578	–	–	N	N	N	–	–	–	–

APPENDIX B: CLUSTER IMAGES

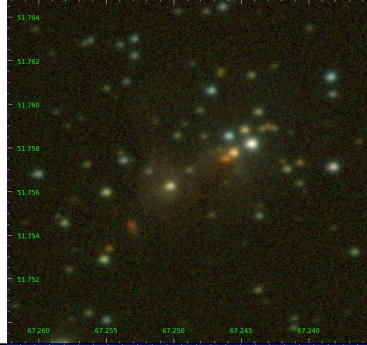

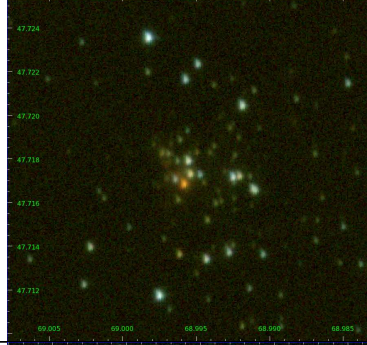
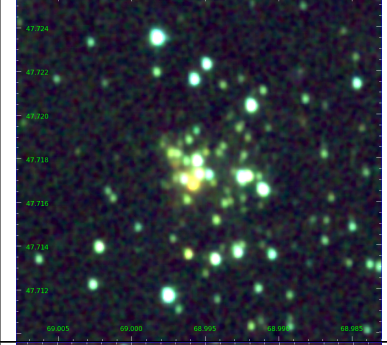
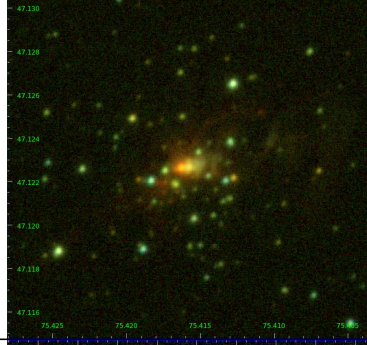
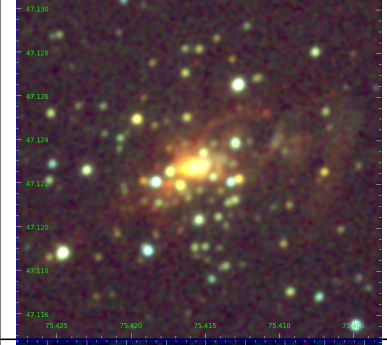

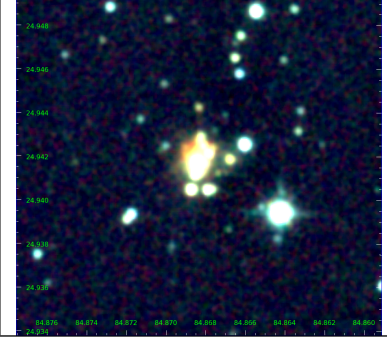
B1 New Clusters

Table B1: Images of the newly detected clusters. We show $JHK(s)$ colour composites from either UGPS or VVV (depending on the cluster position). The image size is $1' \times 1'$, North is up, East is to the left. Images are displayed with two different contrasts to show the various features. The comments column gives a brief description of the cluster and lists associated objects.

MHO	Images		Comments
CI 001			Coincides with IRAS source; dominated by several red stars;
CI 002			Near cluster FSR 0666 but not the same object; known as 2MASX J04055657+5127052, dominated by bright red source and nebulosity;
CI 003			Cluster surrounded by red reflection nebula; Coincides with IRAS source and $20''$ from JCMTSF J040623.4+532201 which is just outside the North-Western edge of the cluster;
CI 004			Rich cluster associated with IRAS, MSX and Maser source; RMS object is classified as HII region;

Continued on next page

Table B1 – continued from previous page

MHO	Images		Comments
CI005			<p>Coincides with IRAS source and nebulosity; 8'' from MSX6C G153.1686+02.1407 and 20'' from GN 04.25.2.01 reflection nebula; elongated (NW to SE) appearance;</p>
CI006			<p>Several bright stars dominate this compact cluster; coincides with IRAS source and 2MASX J04355886+4743034;</p>
CI007			<p>Coincides with IRAS source and 3'' from MSX6C G160.1452+03.1559; known as HII region; extended and filamentary nebulosity throughout the cluster; classified as YSO in RMS survey with a distance of 1.94 kpc;</p>
CI013			<p>Compact cluster coinciding with IRAS source; known HII region GLMP 111 and SiO maser [HLB98] Onsala 52;</p>

Continued on next page

Table B1 – continued from previous page



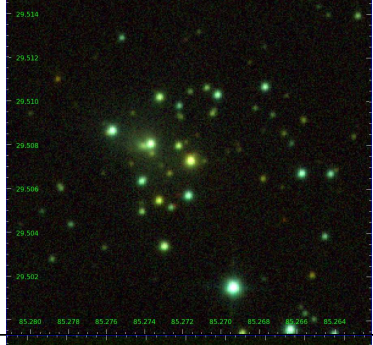

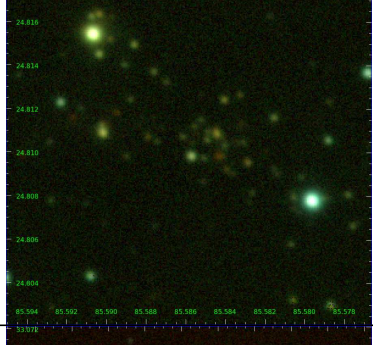
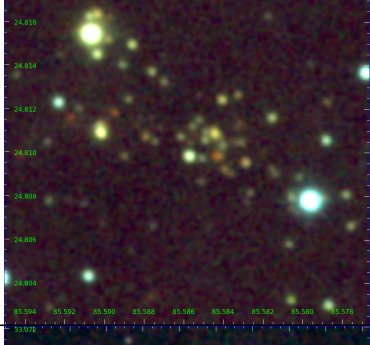
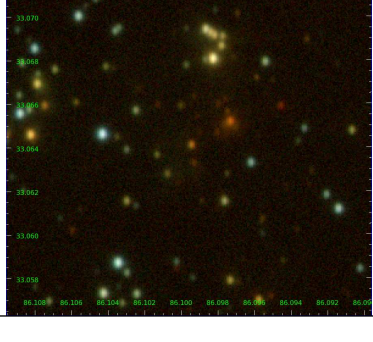
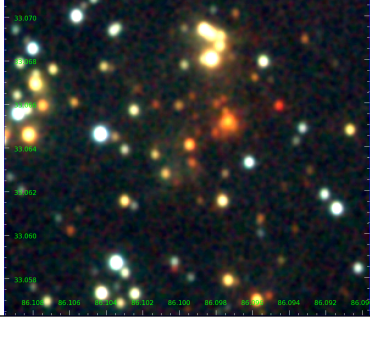
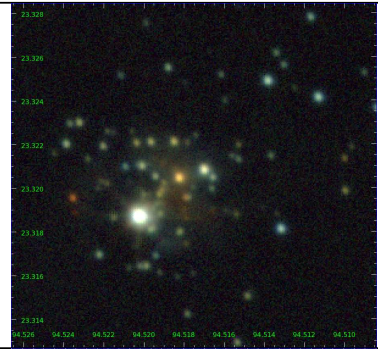
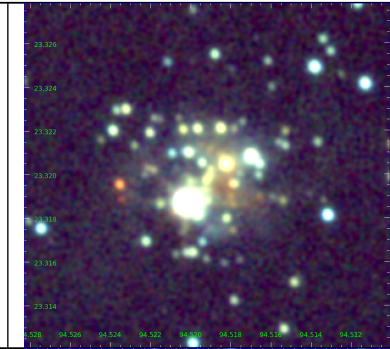

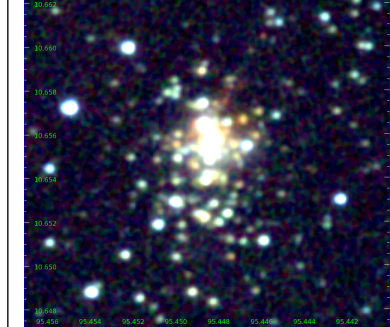
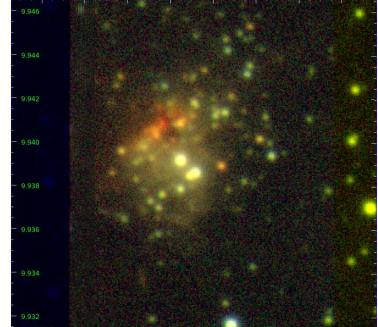
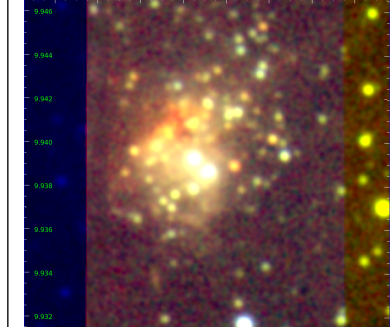
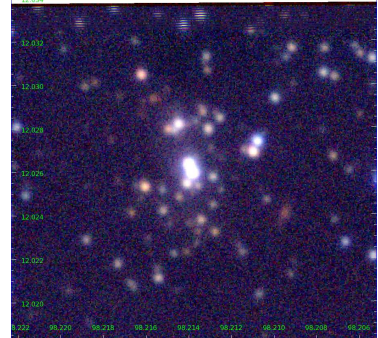
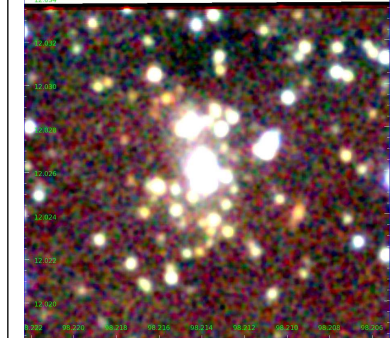
MHO	Images		Comments
CI 014			Sparsely populated cluster coinciding with IRAS source;
CI 015			Coinciding with IRAS source and some faint nebulosity; Coinciding with 2MASX J05410516+2930260;
CI 016			Elongated (North-East to South-West) compact cluster; coinciding with IRAS source and 2MASX J05422061+2448359;
CI 017			Extended cluster with some very red and nebulous objects; Coinciding with IRAS source; 53" from dense core PLCKECC G176.35+01.92;
			Continued on next page

Table B1 – continued from previous page

MHO	Images		Comments
CI 018			Compact cluster coinciding with IRAS source;
CI 019			Cluster surrounding known YSO JCMTSF J055824.5+201349; Coinciding with IRAS source and RMS object with a distance of 2.0 kpc; contains several very red and nebulous objects;
CI 020			Elongated (South-East to North-West) group of stars; bright red star surrounded by nebulosity; known as infrared source 2MFGC 4994;
CI 021			Compact cluster with red nebulous star dominating emission; coinciding with IRAS source;

Continued on next page

Table B1 – continued from previous page

MHO	Images		Comments
CI 022			<p>Cluster dominated by blue star; coinciding with IRAS source; faint nebulosity throughout the cluster;</p>
CI 023			<p>Rich cluster coinciding with an IRAS and RMS object with a distance of 5.78 kpc; 2'' from HII region [UHP2009] VLA G200.0782–01.6333, and YSO MSX6C G200.0789–01.6323;</p>
CI 024			<p>Nebulosity throughout the cluster; some very red sources; coinciding with IRAS and RMS object with a distance of 5.54 kpc; classified as HII region in RMS;</p>
CI 025			<p>Coincident with IRAS source; dominated by two blue-ish stars;</p>


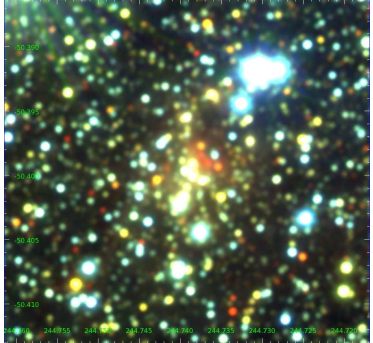
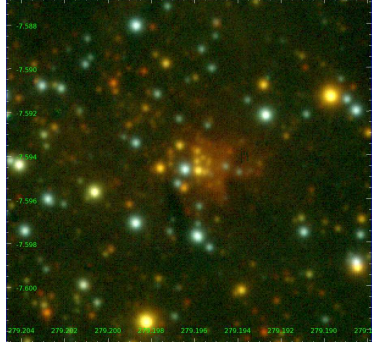
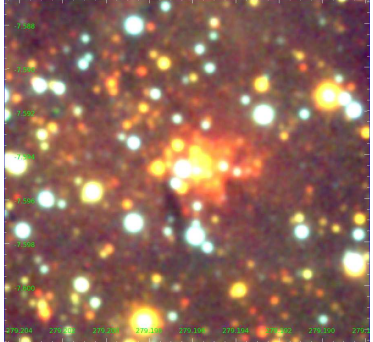
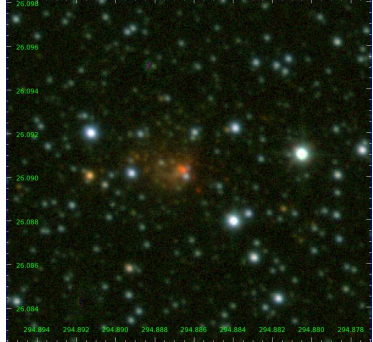

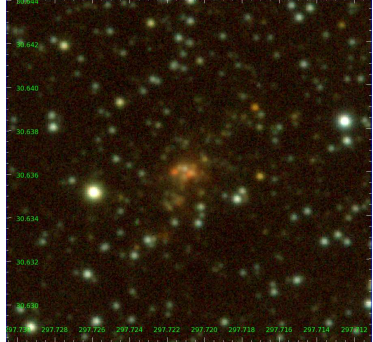

Continued on next page

Table B1 – continued from previous page

MHO	Images		Comments
CI 026			Elongated (North-East to South-West) group of red sources; about 90" from CI 027;
CI 027			Coincident with IRAS source; compact cluster with very red sources and nebulosity; about 90" from CI 026;
CI 028			Small cluster coinciding with IRAS source and identical to 2MASS J06361931+1054263 and ESO-HA 308 emission line star; cluster contains YSO CPM 27 identical to IRAS 06335+1057; within 1 deg of NGC 2264; the hint of nebulosity North of the red NIR source in the cluster is the tip of a bright rimmed cloud;
CI 038			Extended nebulosity with dense filament running through it in absorption; Coinciding with IRAS source and Caswell OH maser 310.146+00.760; identical to 2MASX J13515956-6115394;

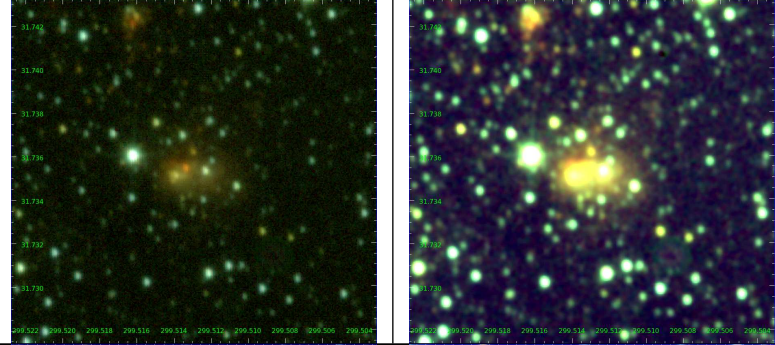
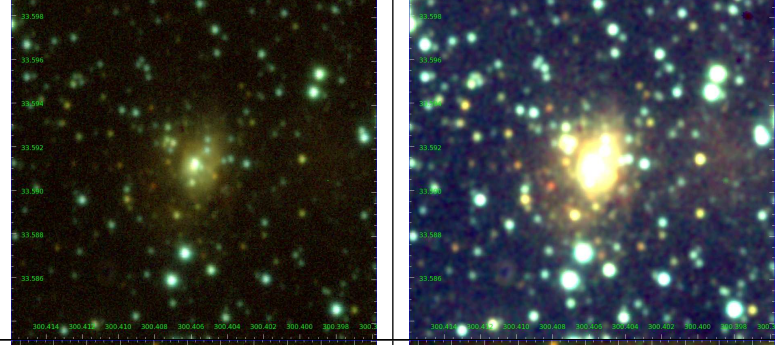
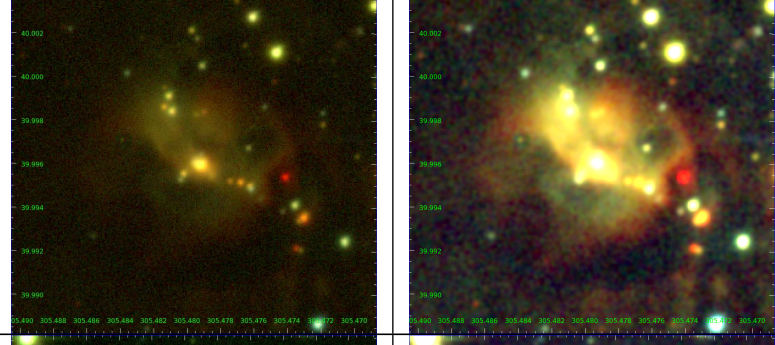
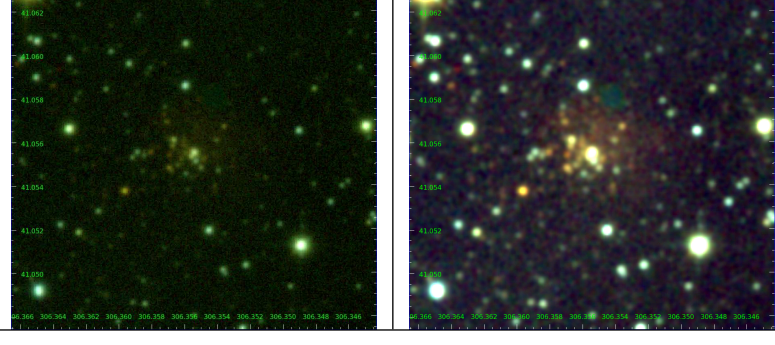
Continued on next page

Table B1 – continued from previous page

MHO	Images		Comments
Cl 039			Identical to MSX5C G333.0297–00.0654; surrounded by nebulosity; 7" from Caswell CH3OH maser 333.029–00.063;
Cl 041			Compact group of red stars coinciding with nebulous IRAS source; several HII regions and bubbles nearby;
Cl 044			Compact cluster of red stars with nebulosity; coincides with IRAS source;
Cl 046			Very compact cluster with red sources; coincident with IRAS source and some nebulosity;

Continued on next page

Table B1 – continued from previous page

MHO	Images	Comments
CI 047		Compact cluster with bright extended nebulosity; coincides with IRAS and RMS source MSX6C G068.3418+01.3138 with a distance of 7.42 kpc; classified as YSO in RMS and known HII region [UHP2009] VLA G068.3414+01.3141;
CI 048		Compact cluster with bright nebulosity; 2'' from YSO MSX6C G070.3164+01.6493; coincides with IRAS and RMS source with a distance of 7.42 kpc;
CI 049		Extended nebulous region with red stars; coincides with RMS source MSX6C G077.8999+01.7678; 3'' from SFR [SUH2012] G077.901+01.769; classified as YSO in RMS with a distance of 1.4 kpc;
CI 050		Cluster with one bright and many fainter members embedded in nebulosity; coincides with IRAS source and 5'' from SFR [SUH2012] G079.151+01.830;

Continued on next page

Table B1 – continued from previous page

MHO	Images	Comments
CI 051		<p>Faint red cluster stars with nebulosity throughout; 3" from YSO MSX6C G078.1952+00.5497; coincident with IRAS and RMS source with distance of 8.51 kpc; classified as HII region in RMS;</p>
CI 053		<p>Bright blue (potentially foreground) object surrounded by red stars and extended nebulosity; coincides with IRAS source and 3" from maser [HLB98] Onsala 136;</p>
CI 054		<p>Bright blue (potentially foreground) stars with red cluster members and extended nebulosity; coincides with IRAS source and 2MASX J20415353+4531596; near cluster CI 055;</p>
CI 055		<p>Several bright red stars dominate brightness; coincides with 2MASX J20415515+4532386; faint nebulosity throughout; near cluster CI 054;</p>

Continued on next page

Table B1 – continued from previous page

MHO	Images		Comments
Cl 056			Compact cluster of faint red stars and nebulosity; coincides with IRAS source;
Cl 057			Compact group of stars surrounded by nebulosity; coincides with IRAS source and HII region Teutsch GN J2046.3+4624;
Cl 058			Several bright red and nebulous members; coincides with IRAS source and RMS object MSX6C G089.2727+01.6703 with distance of 8.06 kpc; same as HII region [UHP2009] VLA G089.2729+01.6703;
Cl 059			Group of several bright stars surrounded by blue and red nebulosity; coincides with IRAS source and RMS object MSX6C G090.7764+02.8281 with distance of 1.74 kpc; potentially HII region but classified in RMS as YSO;

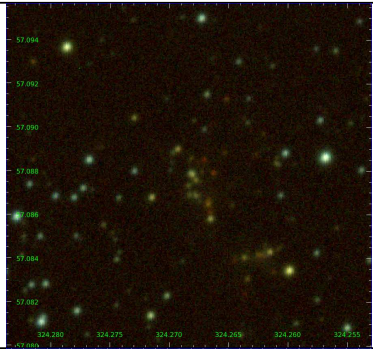
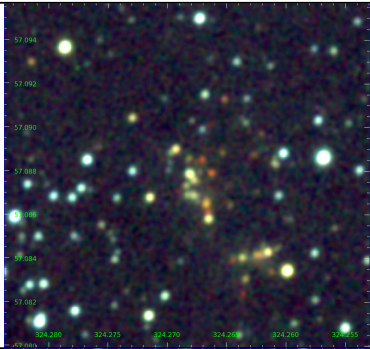
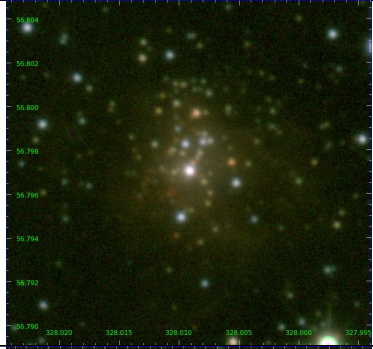
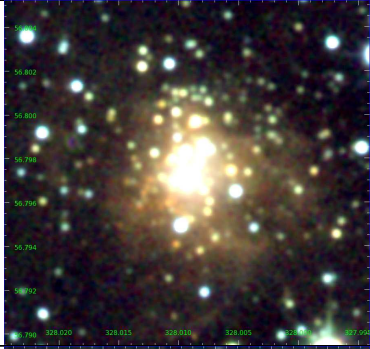
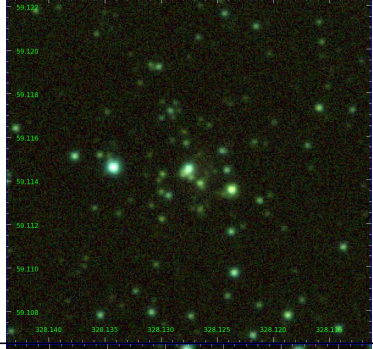

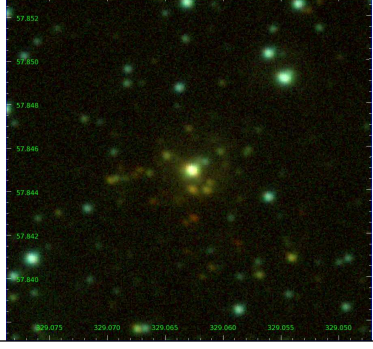
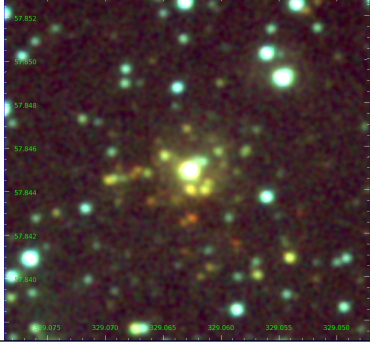
Continued on next page

Table B1 – continued from previous page

MHO	Images		Comments
Cl 060			<p>Small group of red stars coinciding with IRAS and RMS source MSX6C G093.0166+02.4953; classified as HII region in RMS;</p>
Cl 061			<p>Compact cluster dominated by red star; coincides with IRAS source;</p>
Cl 062			<p>Rich cluster with numerous bright stars and nebulosity throughout; coincides with IRAS and RMS source G093.8588+01.5551 with distance of 6.36 kpc; classified as HII region in RMS;</p>
Cl 063			<p>Compact group of stars surrounded by faint nebulosity; coincides with IRAS source;</p>

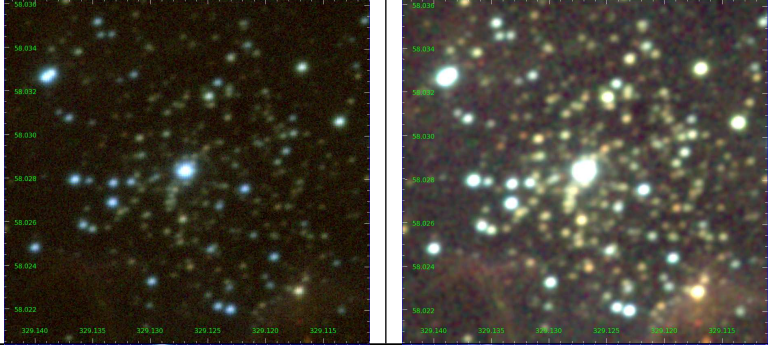
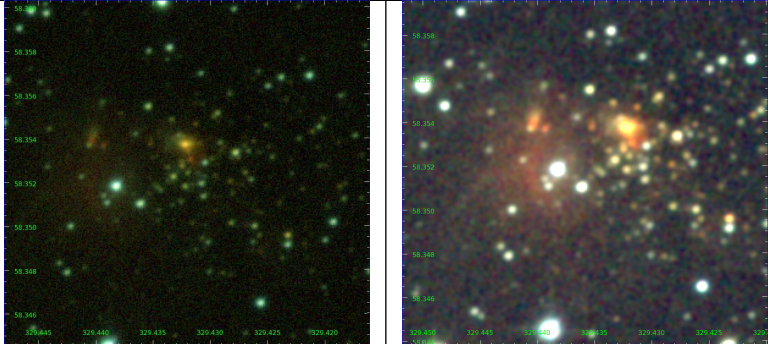
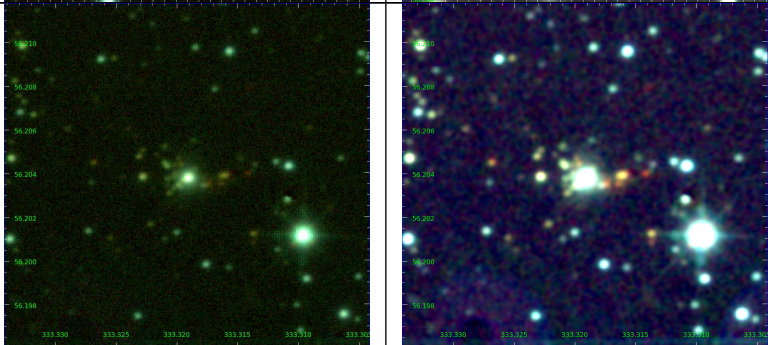
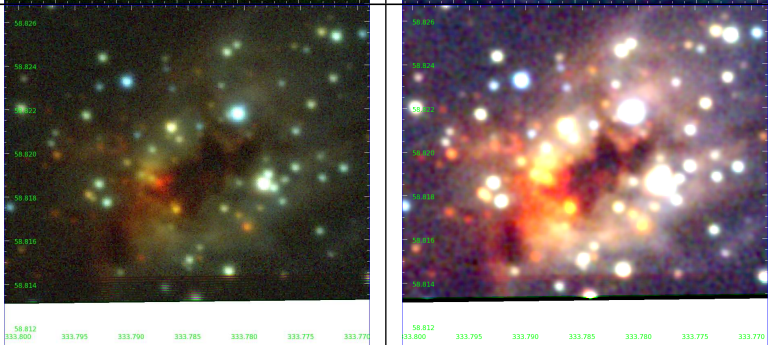
Continued on next page

Table B1 – continued from previous page

MHO	Images		Comments
Cl 064			Compact group of red stars, no obvious nebulosity;
Cl 066			Bright nebulosity throughout the cluster; coincides with IRAS and RMS source with distance of 5.85 kpc; classified as HII region;
Cl 067			Group of faint stars; coincides with IRAS source; no obvious nebulosity;
Cl 068			Cluster of red stars dominated by bright object with some faint nebulosity; coincides with IRAS source;

Continued on next page

Table B1 – continued from previous page

MHO	Images		Comments
CI 069			Central blue bright star surrounded by rich cluster; cluster surrounded by nebulosity; coincides with IRAS source; known HII region WN B2154.8+5747;
CI 070			Extended cluster with in part very red and nebulous stars; coincides with IRAS and RMS source G101.7639+02.8100 with distance 7.81 kpc; classified as HII region in RMS and coincides with maser [GRC90] B215606.0+580645;
CI 071			Very compact, slightly elongated (East-West) group of red stars; dominated by bright central stars with some nebulosity; coincides with IRAS source;
CI 072			Known cluster around IRAS 22134+5834 (Kumar et al. 2003) without SIMBAD entry; counterpart of RMS source MSX6C G103.8744+01.8558 at distance of 1.59 kpc; extended cluster with bright nebulosity and dust lanes; classified as HII region in RMS;

Continued on next page

Table B1 – continued from previous page

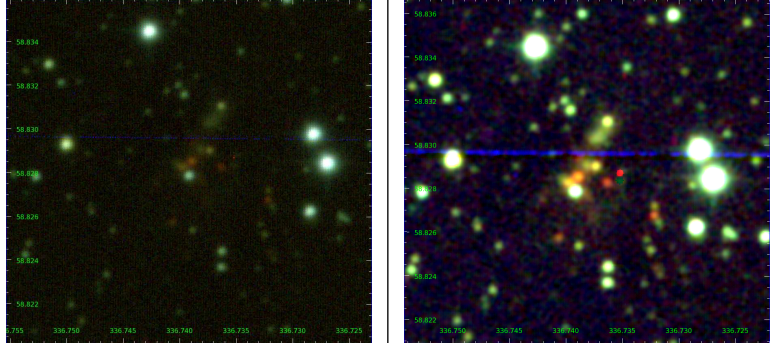
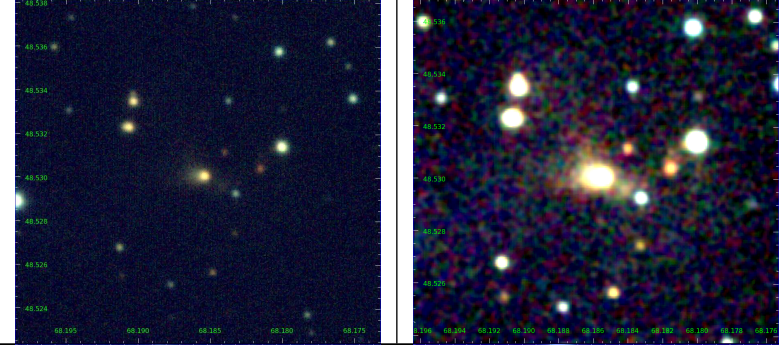
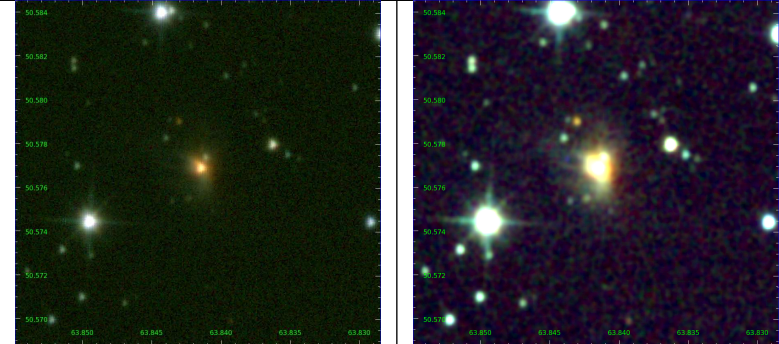
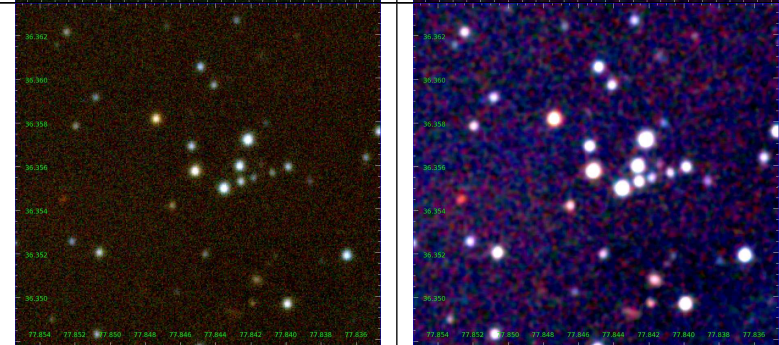
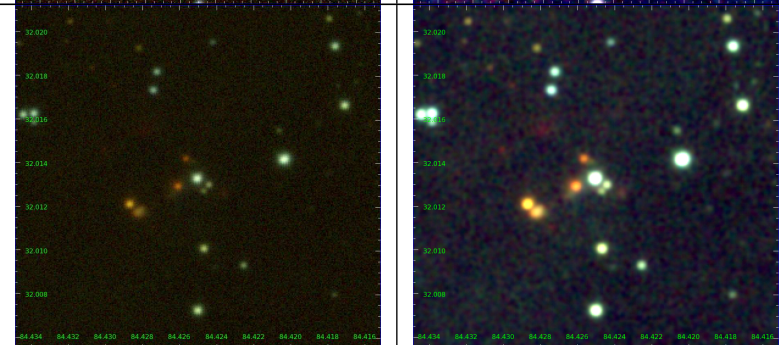
MHO	Images	Comments
CI 075		Small group of red nebulous stars; coincides with IRAS source;

Table B2 – continued from previous page

MHO	Images		Comments
CI082			Nebulous bright red object with some other red stars; coincides with IRAS source;
CI083			Nebulous red object; coincides with IRAS source and 2MASX J04152200+5034364;
CI084			Coincides with IRAS source; group of similar colour and brightness stars; potentially asterism;
CI085			Group of red stars near cluster [FMT2009] 11 or NGC 1985 IR; several IR/smm/rad sources within 20";

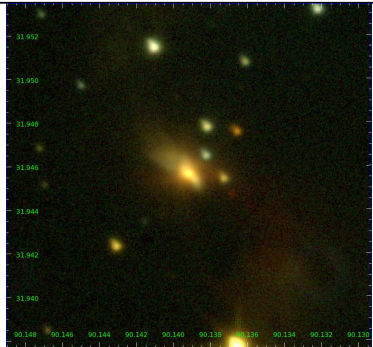
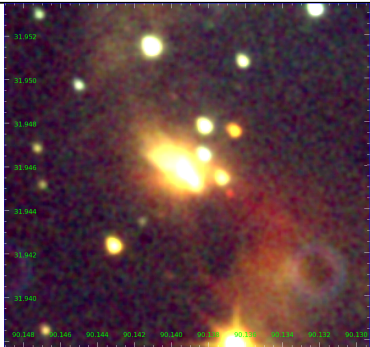
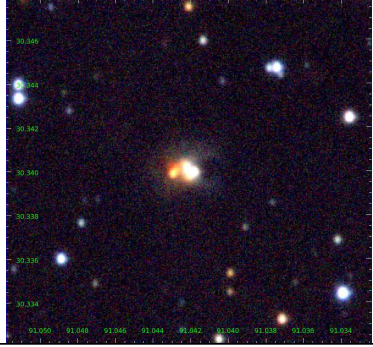

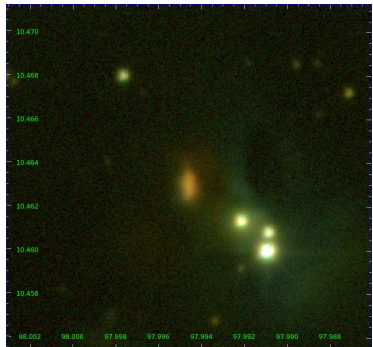

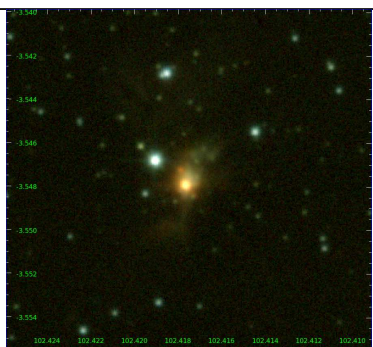

Continued on next page

Table B2 – continued from previous page

MHO	Images		Comments
CI 086			Group of stars near cluster [FMT2009] 11 or NGC 1985 IR; potential asterism;
CI 087			Nebulous YSO 2MASS J05470434+2059415; identical to HH 290 IRS;
CI 088			Red nebulous source coinciding with maser and IRAS 05466+2316;
CI 089			Group of stars dominated by very bright OH/IR star IRAS 05506+2414; surrounded by bright reflection nebula; coincides with RMS source G184.9551-00.8559 at distance of 3.66 kpc; classified as Young/Old star in RMS;

Continued on next page

Table B2 – continued from previous page

MHO	Images		Comments
CI 090			Group of red stars dominated by bright nebulous object; coincides with IRAS source and RMS object G179.0380+04.3003 with distance of 1.1 kpc; classified as YSO in RMS;
CI 091			Nebulous objects; coincides with IRAS source;
CI 092			Several nebulous bright objects; coincides with IRAS source;
CI 093			Cluster dominated by bright red nebulous object; coincides with IRAS source;

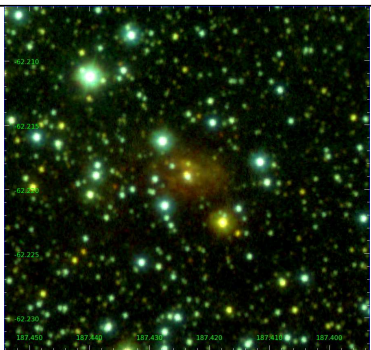
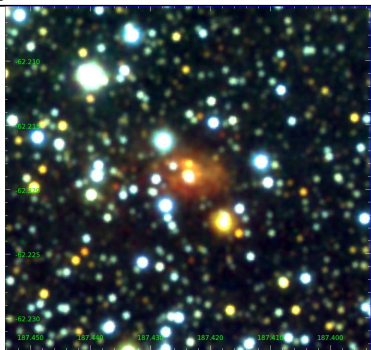
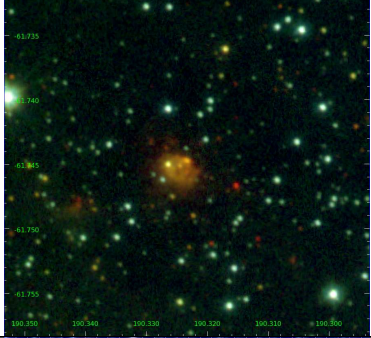



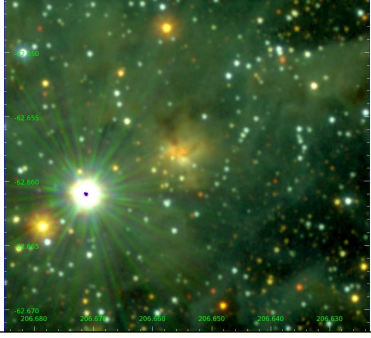
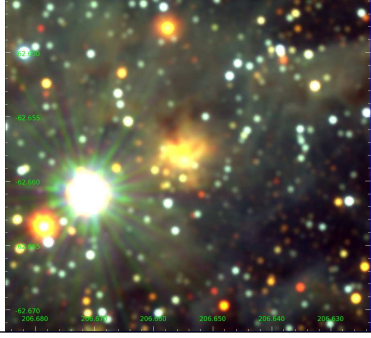
Continued on next page

Table B2 – continued from previous page

MHO	Images	Comments
CI 095		<p>Dominated by nebulous YSO 2MASX J07042156–1623197; 5'' from MSX6C G228.9946–04.6200; 10'' from IRAS 07020-1618;</p>
CI 096		<p>Nebulous YSO IRAS 07100–1110; 2'' from HII region MSX6C G225.3266–00.5318;</p>
CI 097		<p>Nebulosity throughout extended group of faint red stars; coincides with YSO IRAS 11426–6301;</p>
CI 098		<p>Very red source surrounded by extended nebulosity; coincides with IRAS source and known bubbles nearby;</p>

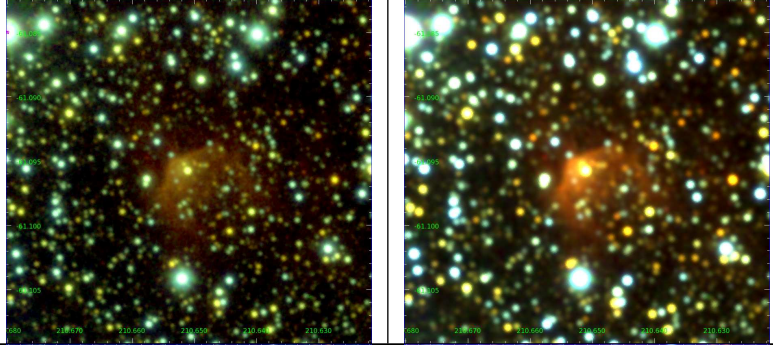
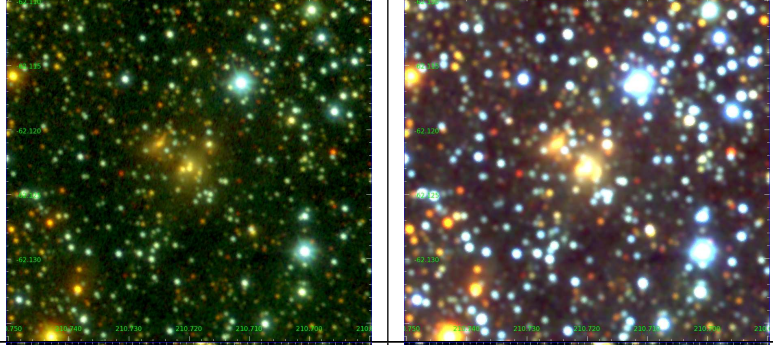
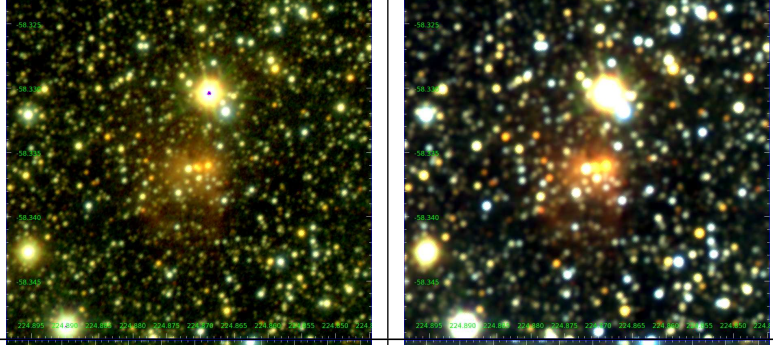
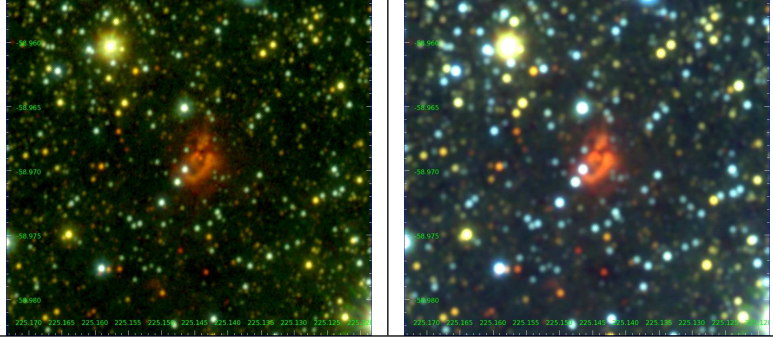
Continued on next page

Table B2 – continued from previous page

MHO	Images		Comments
CI 099			Red nebulous source; coincides with IRAS source; known bubbles nearby;
CI 100			several red sources embedded in bright nebosity; coincides with YSO IRAS 12383–6128; several sub-mm sources nearby;
CI 101			Red stars embedded in nebosity; 1" from YSO candidate [MHL2007] G308.0314–01.0529 1; coincides with IRAS source;
CI 102			Coincides with IRAS source and 2MASX J13463702–6239303; surrounded by very extended nebosity;

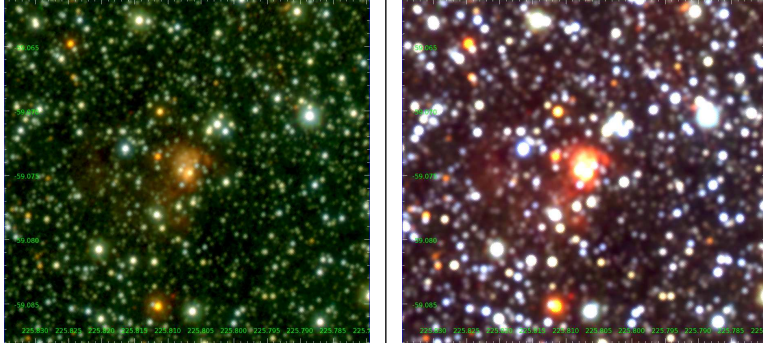
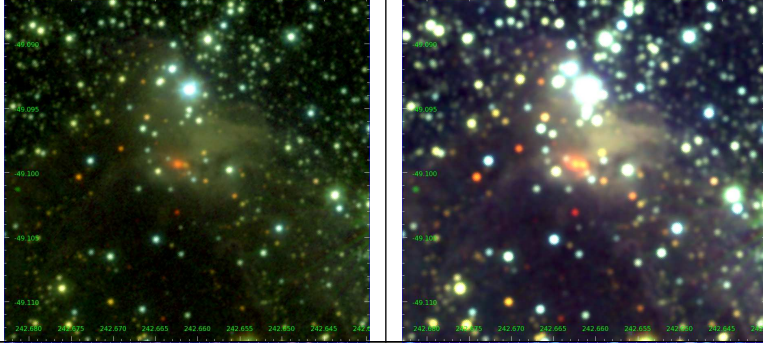
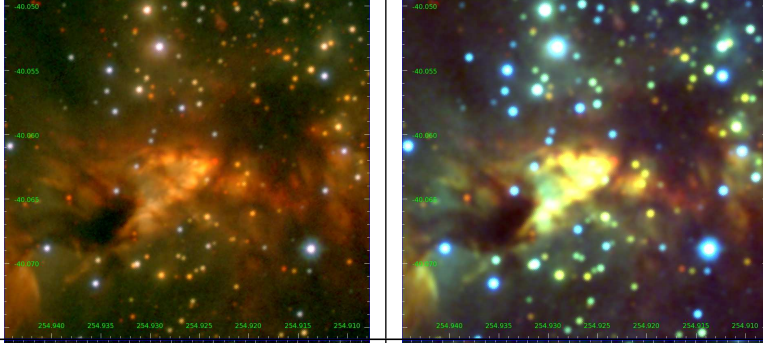
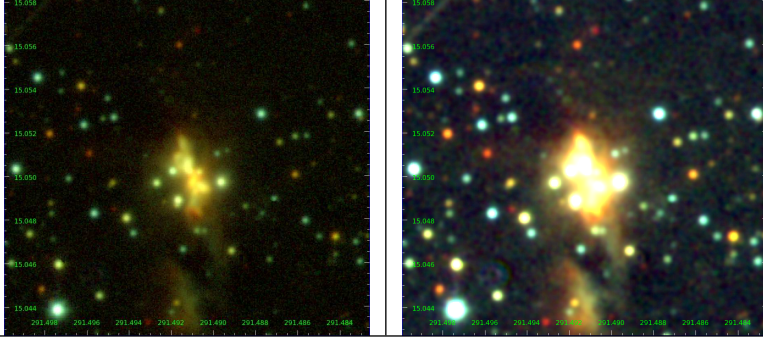
Continued on next page

Table B2 – continued from previous page

MHO	Images	Comments
CI 103		<p>Bright red star surrounded by red nebulosity; coincides with IRAS source; several bubbles and HII regions nearby;</p>
CI 104		<p>Coincides with IRAS source and 2MASS J14025282–6207226; compact group of red and slightly nebulous sources;</p>
CI 105		<p>Compact group dominated by three bright red stars with some nebulosity; coincides with IRAS source;</p>
CI 106		<p>Coincides with 2MASX J15003503–5858101 and MSX6C G318.9148–00.1647; surrounded by red nebulosity; 14'' from maser [CBJ88] 145645.1–584623; known bubble and HII region;</p>

Continued on next page

Table B2 – continued from previous page

MHO	Images	Comments
CI 107		<p>Red central star surrounded by nebulosity; known HII region IRAS 14593–5852 and MSX6C G319.1632–00.4208; nearby bubble and YSOs;</p>
CI 108		<p>Several very red sources within extended nebulosity; known HII region IRAS 16069–4858; 6'' from MSX6C G332.9565+01.8035;</p>
CI 109		<p>Coincides with nebulous YSO candidate IRAS 165624–3959; 5'' from maser [HLB98] SEST 119;</p>
CI 110		<p>Very nebulous red sources; known HII region IRAS 19236+1456 and MSX6C G050.2213–00.6063 with distance from RMS of 3.34 kpc;</p>

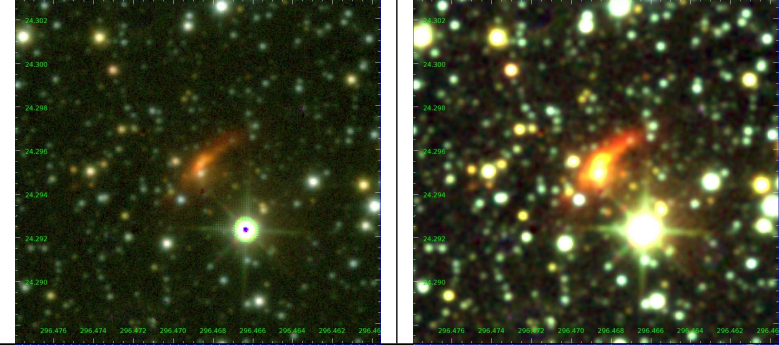
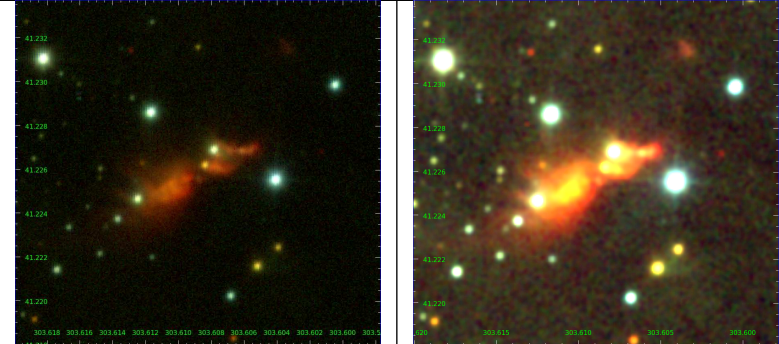
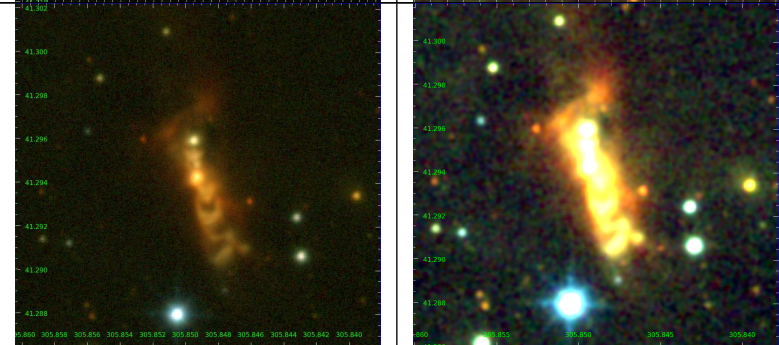
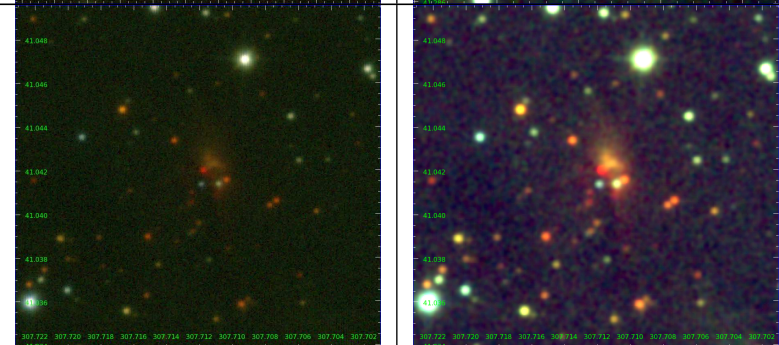
Continued on next page

Table B2 – continued from previous page

MHO	Images	Comments
CI 111		<p>Red nebula around IRAS 19253+1748 and RMS source MSX6C G052.9217+00.4142; classified as maser in RMS with distance of 5.06 kpc;</p>
CI 112		<p>Red central source with bipolar red nebula; known YSO MSX6C G052.9221–00.4892; coincides with IRAS source and RMS object with distance of 5.06 kpc;</p>
CI 113		<p>Compact group of red stars and nebula; coincides with IRAS source and RMS object MSX6C 052.9190–00.8610; ATLASGAL match has vlsr of 56.1 km/s;</p>
CI 114		<p>Compact group of red and faint stars with some nebula; coincides with IRAS source;</p>

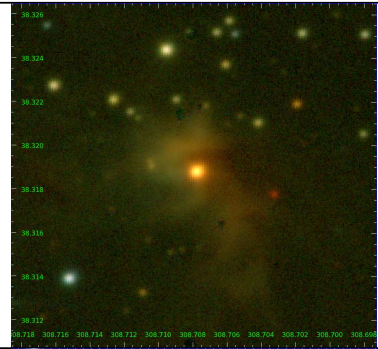
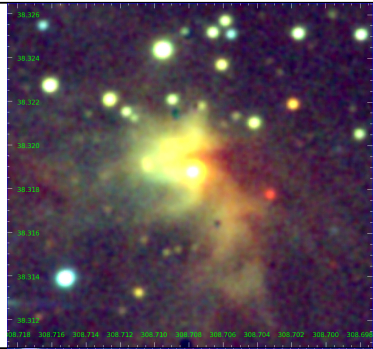
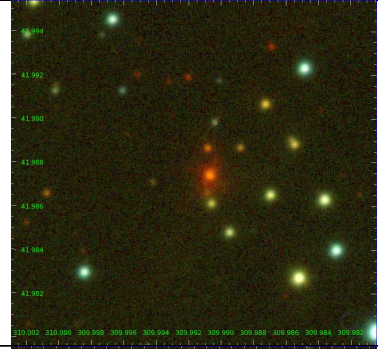
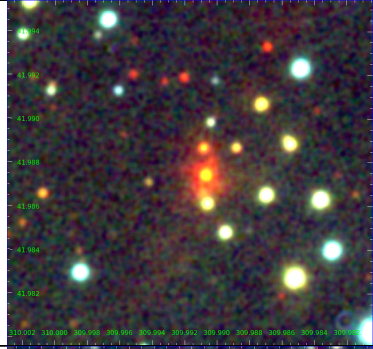
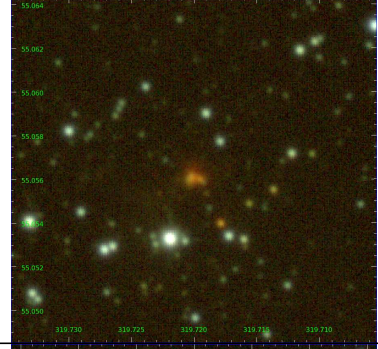

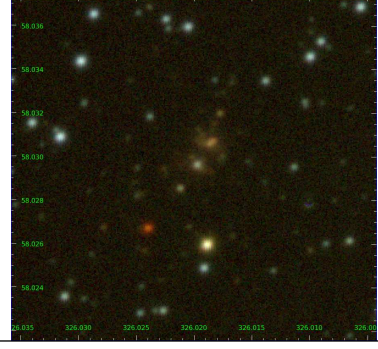
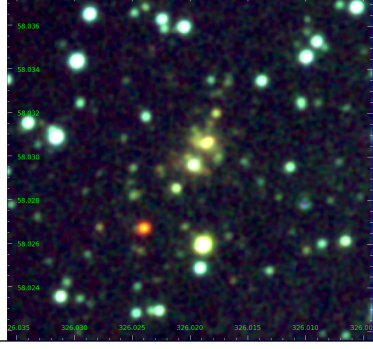
Continued on next page

Table B2 – continued from previous page

MHO	Images		Comments
CI 115			Very red nebula near IRAS 19437+2410; 2'' from HII region MSX6C G060.5750–00.1861; classified as YSO in RMS with distance of 7.48 kpc;
CI 116			Bipolar nebula surrounding YSO IRAS 20126+4104; driving source of MHO 860; 8'' from maser [ZHS99] 201240.210+410426.53; classified as YSO in RMS with distance of 1.4 kpc;
CI 117			Bipolar nebula from HII region MSX6C G079.1272+02.2782 which is potential outflow; coincides with IRAS source; classified as YSO in RMS with distance of 1.4 kpc;
CI 118			Several red sources with surrounding nebula; identical to MSX5C G079.7361+00.9904 and coinciding with IRAS source; 5'' from maser [BK2004] J203050.8+410225;

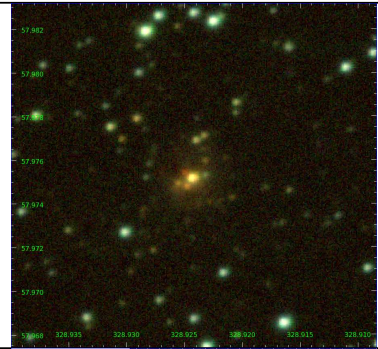
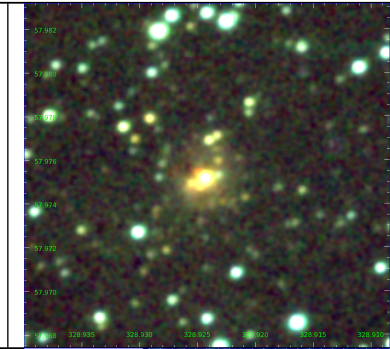
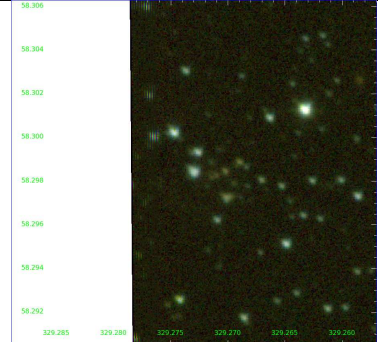
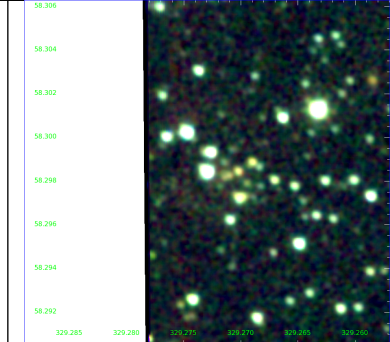
Continued on next page

Table B2 – continued from previous page

MHO	Images		Comments
Cl 119			<p>Dominated by bright red source surrounded by nebulosity; known as YSO MSX6C G078.0013–01.244; coinciding with IRAS source;</p>
Cl 121			<p>Red nebulous HII region MSX6C G081.5168+00.1926; 3" from SFR [SUH2012] G081.516+00.192; coinciding with RMS source with distance of 1.4 kpc; classified as YSO;</p>
Cl 122			<p>Several red nebulous objects; coinciding with IRAS source; 5" from H₂O maser [GRC90] B211721.2+545037;</p>
Cl 123			<p>Dominated by two bright sources with faint nebulosity; coincident with IRAS source;</p>

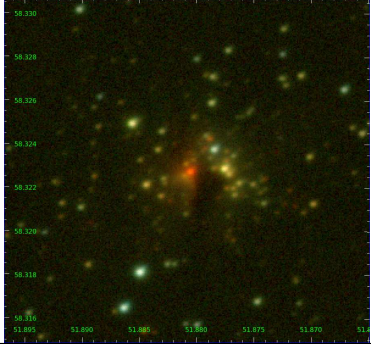
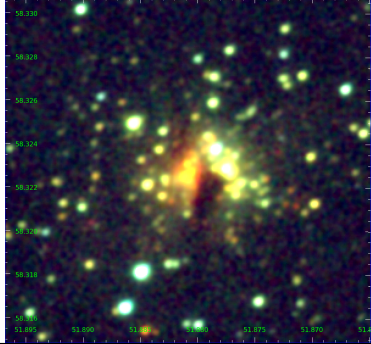
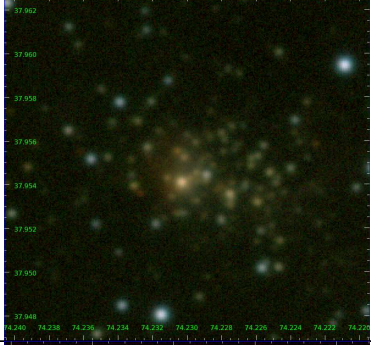
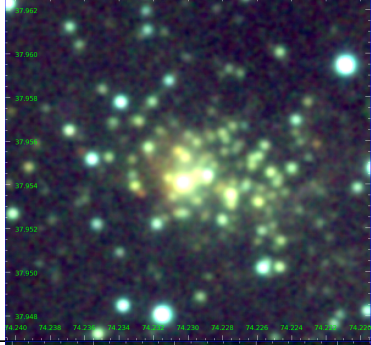
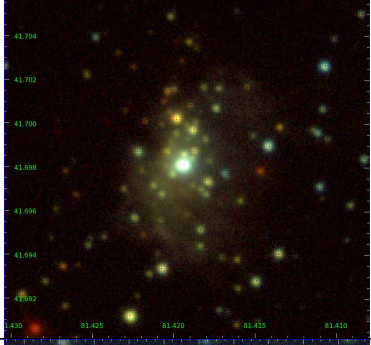

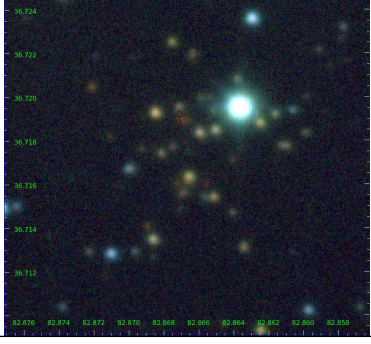
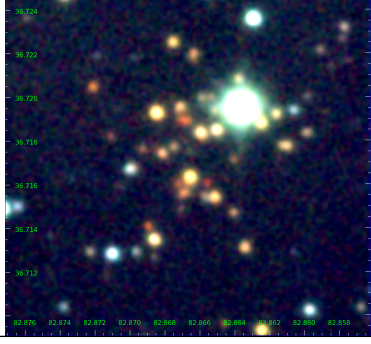
Continued on next page

Table B2 – continued from previous page

MHO	Images		Comments
CI 124			<p>Dominated by bright red source with some nebulosity; classified as PN PM 1-335; coinciding with IRAS source and RMS object MSX6C G101.3193+02.6785; classified as YSO in RMS with distance of 6.24 kpc;</p>
CI 125			<p>Compact group of faint stars; coinciding with IRAS source;</p>

B3 Known Cluster Candidates

Table B3: As Fig. B1, but for the known cluster candidates.

MHO	Images		Comments
Confirmed Clusters			
CI 126			Rich cluster with nebulosity and dust lanes; known as [SUH2012] G142.244+01.429; coincides with IRAS source and RMS object MSX6C G142.2446+01.4299; 90'' from [SUH2012] G142.2184+01.432; classified as HII region in RMS with distance of 4.15kpc;
CI 127			Rich cluster with some faint nebulosity; known as [SUH2012] G166.813-03.200; coincides with IRAS and RMS source G166.8141-03.1986; classified as HII region in RMS with distance of 2.0 kpc;
CI 128			Dominated by bright blue stars and nebulosity; known as [SUH2012] G167.060+03.464; coincides with IRAS source;
CI 129			Small cluster of red stars; known as [SUH2012] G171.8344+01.644;

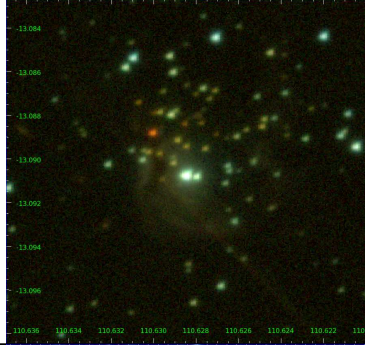
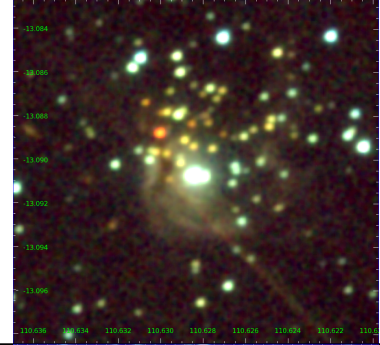
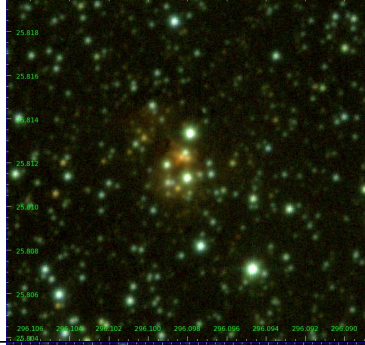
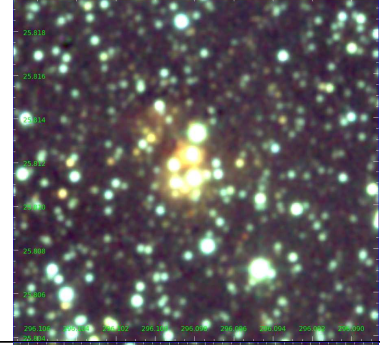
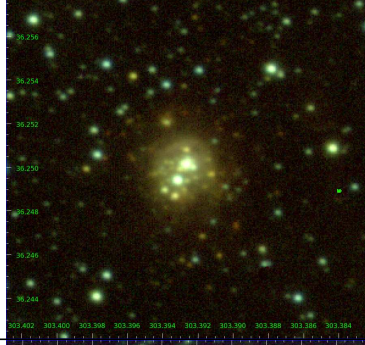

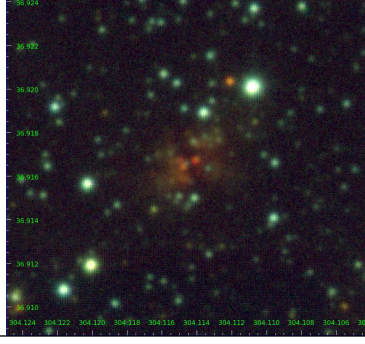
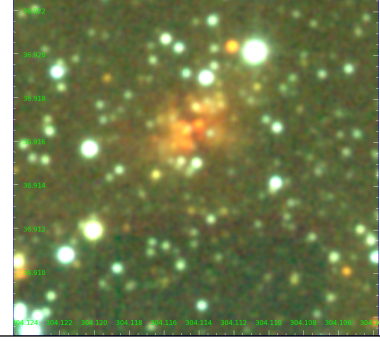
Continued on next page

Table B3 – continued from previous page

MHO	Images		Comments
CI 130			Small cluster of red stars; known as [SUH2012] G171.8534+01.637;
CI 131			Dominated by bright star with nebulosity; known as [IBP2002] CC11; classified as potential globular cluster - given the nebulosity and the UKIDSS images this is clearly not the case; coincides with IRAS source;
CI 132			Small group of red stars; known as [SUH2012] G210.469-02.339; coincides with IRAS source;
CI 133			Extended group of faint red stars; known as [SUH2012] G210.415-01.960; coincides with IRAS source;

Continued on next page

Table B3 – continued from previous page

MHO	Images		Comments
CI 134			<p>Cluster of red stars dominated by two blue stars surrounded by nebulosity; known as [SUH2012] G228.098+00.797; coincides with IRAS source; classified as PN candidate PN G228.1+00.8 in MASH - given the UKIDSS images this is more likely an HII region;</p>
CI 135			<p>Compact cluster of stars with some nebulosity; known as [SUH2012] G061.720+00.863; coincides with IRAS source; classified as HII region G061.7201+00.8630 in RMS survey with distance of 13.99 kpc;</p>
CI 136			<p>Compact cluster of red stars with bright nebulosity; known as [SUH2012] G073.878+01.026; coincides with IRAS source; classified as HII region G073.8775+01.0245 in RMS survey with distance of 9.28 kpc;</p>
CI 137			<p>Red central object with bipolar nebulosity; known as [SUH2012] G074.753+00.913; coincides with IRAS source; classified as HII region G074.7541+00.9132 in RMS with a distance of 9.29 kpc;</p>

Continued on next page

Table B3 – continued from previous page

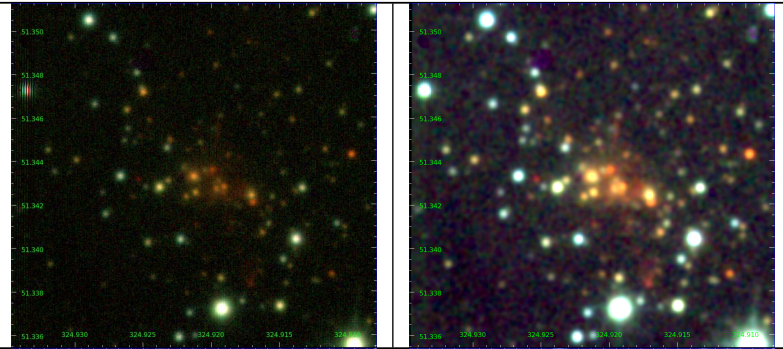
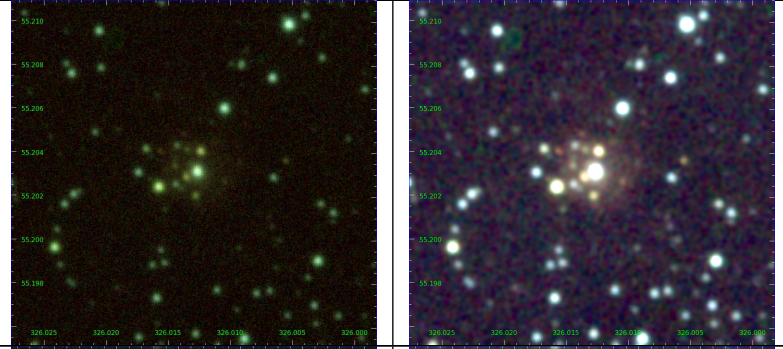
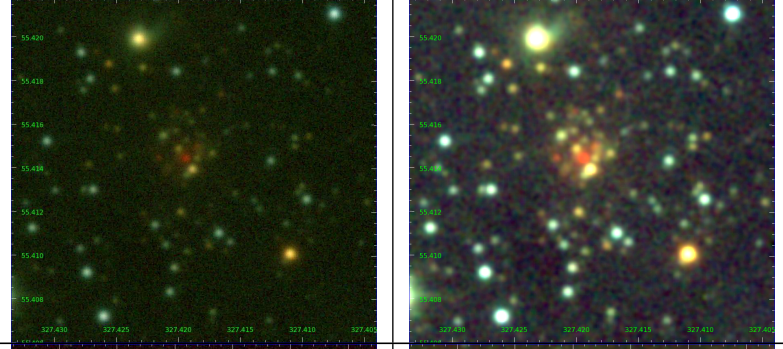
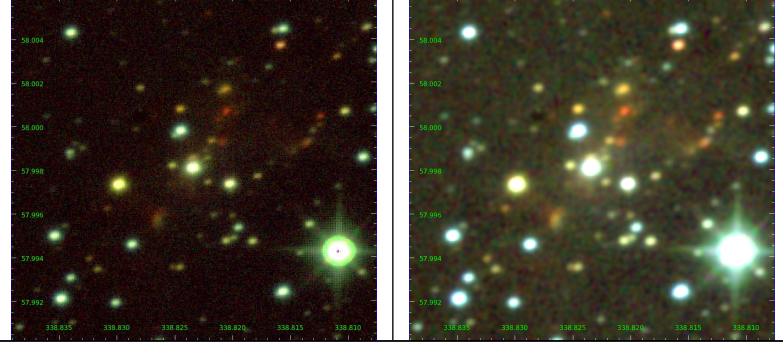
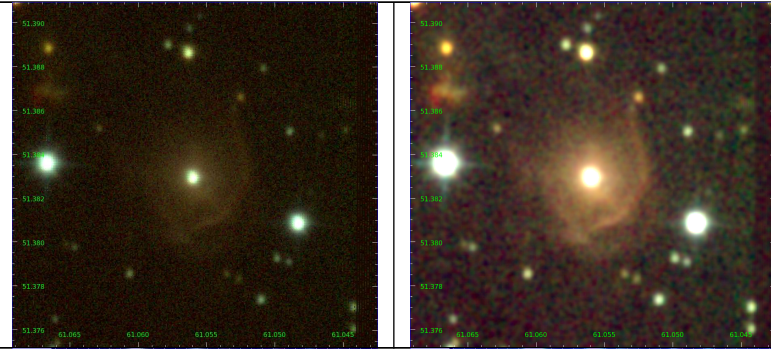
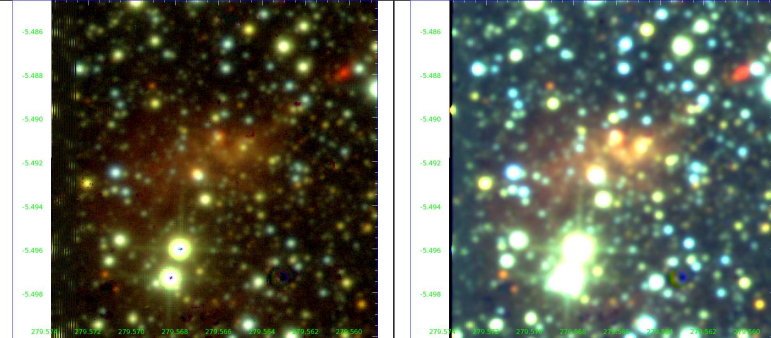
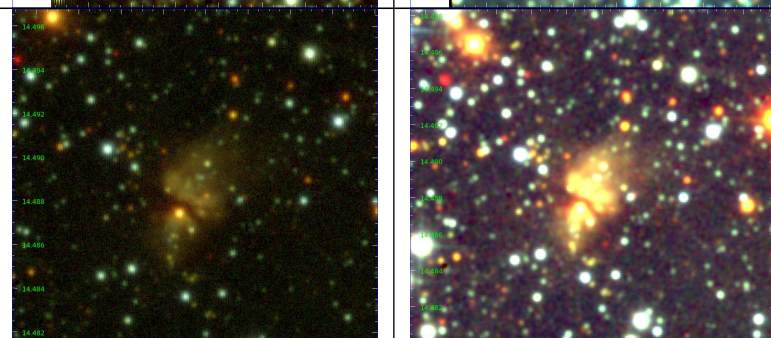
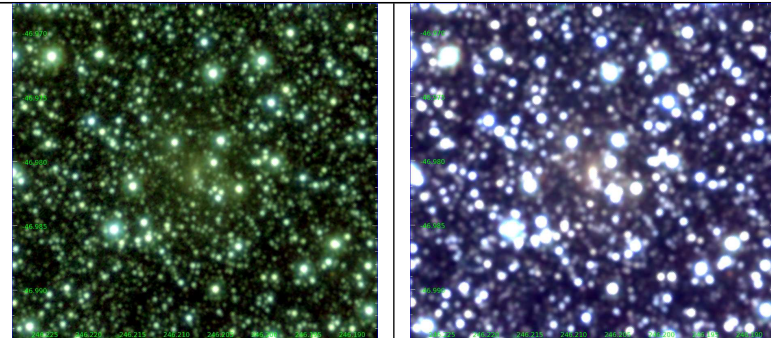
MHO	Images		Comments
CI 138		<p>Cluster of red stars with some nebulosity; known as [SUH2012] G095.296–00.937; coincides with IRAS source and maser;</p>	
CI 139		<p>Compact cluster of stars surrounded by faint nebulosity; known as [SUH2012] G098.320+01.551; coincides with IRAS source;</p>	
CI 140		<p>Compact cluster of red stars; known as [SUH2012] G099.070+01.200; coincides with IRAS source;</p>	
CI 141		<p>Distributed group of red stars with some faint nebulosity; known as [SUH2012] G105.675–00.237; coincides with IRAS source;</p>	
Continued on next page			

Table B3 – continued from previous page

MHO	Images		Comments
Unconfirmed Cluster candidates			
CI 142		Single star surrounded by nebulosity; known as Camargo 442; coincides with IRAS source; no clear cluster detectable;	
CI 143		Red nebulous region; known as [SUH2012] G026.544+00.414; coincides with IRAS source; no clear cluster detectable;	
CI 144		Bright bipolar nebulosity with dark dust lane around red star; known as [SUH2012] G049.288–00.056; coincides with IRAS source and RMS object; classified as YSO in RMS at distance of 5.4 kpc; no clear cluster detectable, but given the large distance this is not surprising;	

B4 Unknown Object

Table B4: As Fig. B1, but for the object that cannot be classified.

MHO	Images		Comments
CI 145		Apparent increase in projected stellar density in crowded field which could be a cluster; the object FSR 1735 - now confirmed as a globular cluster - had a similar appearance in 2MASS data;	